Robustness of the quantum Hall effect, sample size versus sample topology, and quality control management of III-V molecular beam epitaxy

Ralf D. Tscheuschner,* Sascha Hoch, Eva Leschinsky,
Cedrik Meier, Sabine Theis, and Andreas D. Wieck

Angewandte Festkörperphysik

Ruhr-Universität Bochum

Universitätsstraße 150

D-44780 Bochum

Federal Republic of Germany

February 1, 2008

Abstract

We measure the IQHE on macroscopic ($1.5\,\mathrm{cm} \times 1.5\,\mathrm{cm}$) "quick and dirty" pre-pared III-V heterostucture samples with van der Pauw and modified Corbino geometries at 1.3 K. We compare our results with (i) data taken on smaller specimens, among them samples with a standard Hall bar geometry, (ii) results of our numerical analysis taking inhomogenities of the 2DEG into account. Our main finding is a confirmation of the expected robustness of the IQHE which favours the development of wide plateaux for small filling factors and very large samples sizes (here with areas $10\,000$ times larger than in standard arrangements).

---

*_permanent e-mail address:_ ralfd@provi.de

Contents

1   Introduction and theoretical perspective

A remarkable fact is that the inverse VON KLITZING constant [1]

$$\frac{1}{R_{vK}} = \frac{e^2}{h} = \frac{e}{h/e} \tag{1}$$

is nothing but a ratio between an elementary electric and an elementary magnetic quantity, namely the elementary electronic charge and the LONDON magnetic flux quantum.[1] This is not unlike the expression for the vacuum impedance

$$Z_0 = \sqrt{\frac{\mu_0}{\varepsilon_0}}, \tag{2}$$

the fundamental quantity of r.f. technology. In fact, the fundamental constant of quantum electrodynamics, the SOMMERFELD fine structure constant, is given by the ratio (in MKSA units)

$$\alpha = \frac{Z_0}{2R_{vK}} = \frac{\sqrt{\mu_0/\varepsilon_0}}{2\,h/e^2} = \frac{e^2}{4\pi\varepsilon_0\,\hbar c} = \frac{e^2\mu_0 c}{4\pi\hbar}. \tag{3}$$

More strikingly, the ratio g/e between the charge of a hypothetical DIRAC magnetic monopole [2] and an electron charge is supposed to be

$$\frac{g}{e} = \frac{Z_0}{2\alpha} = R_{vK}, \tag{4}$$

since the DIRAC quantization condition for a configuration consisting of an elementary electric charge e and an elementary magnetic charge g reads (in MKSA)

$$\frac{1}{\hbar c} \cdot \frac{g}{\sqrt{4\pi\mu_0}} \cdot \frac{e}{\sqrt{4\pi\varepsilon_0}} = \frac{1}{2}. \tag{5}$$

Notice, in terms of GAUSSian quantities we have to write instead

$$\alpha = \frac{e^2}{\hbar c}, \qquad \frac{g}{e} = \frac{1}{2\alpha}, \qquad \frac{g \cdot e}{\hbar c} = \frac{1}{2}. \tag{6}$$

"The VON KLITZING resistance is an universal ratio between a magnetic and an electric quantity." This statement suggests that the quantum HALL effect is a truly fundamental

---

[1] "LONDON magnetic flux quantum h/e" as opposed to the "BCS magnetic flux quantum $h/2e$" reflecting the fact that the electrons, from which the superconducting ground state is built, are paired.

phenomenon of quantum electrodynamics contrary to the popular belief prevalent in semi-conductor physics [3, 4, 5, 6, 7].[2] In particular, it implies that the transversal conductivity plateaus appearing at integer (resp. odd rational) multiples of e^2/h reflect a macroscopic quantum state exhibiting a certain range of rigidity against a variation of external parameters such as the strength of the magnetic field or the density of charge carriers. However, unlike BCS superconductivity (including high-T_C superconductivity), here we do not encounter a Bose-like condensate made up from paired electric charges, i.e. the electrons (or holes), but, obviously, a Bose-like condensate made up from flux-charge composites[3] [9, 10, 11, 12]. Let us briefly recall the essence of the argument.

The state characterized by a filling factor $\nu = 1$ may be regarded as an assembly of bound states, each made up from a point-like electric charge e and an infinite thin magnetic solenoid carrying a flux quantum h/e. The cumulative AHARONOV-BOHM-AHARONOV-CASHER (ABAC) [13, 14] phase for adiabatically looping one bound state around another is equal to

$$q.m.\,phase\,shift\,(\text{charge around vortex}) \cdot q.m.\,phase\,shift\,(\text{vortex around charge})$$
$$= \exp\left\{\frac{i}{\hbar}\,e\,(h/e)\right\} \cdot \exp\left\{\frac{i}{\hbar}\,(h/e)\,e\right\} = \exp\left\{\frac{i}{\hbar}\,2\,e\,(h/e)\right\} = \exp i4\pi = 1, \quad (7)$$

where, as usual, we have set $\hbar = h/2\pi$.

A simple exchange of two bound states, interpreted as an exchange of indistinguishable particles in the sense of quantum mechanics, is topologically equivalent to one half of the

---

[2]For example, HALDANE and CHEN strongly argue against this view [8]. They consider the material independence of the QHE a strong evidence *against* electrodynamics effects. They state that then in a physical realistic situation the effect would depend on a material dependent "effective fine structure constant" $\alpha' = (\mu/\varepsilon)^{1/2}/2R_{vK}$. However, quantum physical quantization rules always manifest themselves in terms of bare (microscopic) quantities. One prominent example is the quantization of circulation in neutral superfluids which only depend on the bare mass (of the helium atoms for example) in spite of the strong renormalization effects. (Thanks one extended to Professor NILS SCHOPOHL for reminding us of this point.)

[3]This interpretation is based on the composite boson model by ZHANG, HANSON, and KIVELSON for the fractional effect, but it works for the integer one as well. (For a theoretical framework providing a *unified* description of the integer and fractional quantum HALL effects the reader is refered to JAINs work [9].)

above operation, such that the statistics parameter becomes

$$\exp i\theta = \exp \left\{ \frac{i}{\hbar} e \left(h/e \right) \right\} = \exp i2\pi = 1, \tag{8}$$

where we assumed that the constituents, the electric as well as the magnetic ones, are all bosons. It follows immediately that the composites are bosons at least in a long-distance limit.

However, if we try to incorporate these objects into an action principle, i.e. into a Lagrangian framework, things change dramatically: The composites become fermions, or, if they are built from fermionic electric charges (as electrons are) and bosonic flux lines, they transmute to bosonic charge-flux composites. Let us explain how this happens. The Lagrangian function for an assembly of electrically charged point-like particle in an external electromagnetic potential is given by

$$L = L_{kin} - V(\mathbf{x}_\alpha) + \sum_\alpha \dot{\mathbf{x}}_\alpha \cdot \mathbf{A}(\mathbf{x}_\alpha) = L_{kin} - \sum_\alpha \frac{dx_\mu^\alpha}{dt} A^\mu, \tag{9}$$

with x_μ and A_μ being the space-time coordinate and the electromagnetic 4-potential, respectively. The attachment of a flux line Φ to an electric charge may Q be viewed as an additional constraint, say

$$Q \propto \Phi, \tag{10}$$

such that for the elementary quanta the relation

$$e = \frac{1}{R_{vk}} \cdot \frac{h}{e}. \tag{11}$$

is fulfilled. In an oversimplified language of mathematical physics, where we set $\hbar = h/2\pi = 1$ as well as $e = 1$, the celebrated VON KLITZING resistance is simply 2π, and the constraint has to be rewritten as

$$Q = \frac{1}{2\pi} \cdot \Phi. \tag{12}$$

This is a poor man's form[4] of the CHERN-SIMONS relation [10, 11, 12]. Expressed in terms of the associated densities, e.g. for one pointlike composite at the origin,

$$\varrho_{2D}(x, y) = \delta(x)\delta(y) \tag{13}$$

$$B_z(x, y) = 2\pi\delta(x)\delta(y) \tag{14}$$

[4]freespoken after a joke by P.W. ANDERSON on the renormalization group analysis of the KONDO problem.

we have

$$\int \varrho_{2D} \, d^2x \;=\; \frac{1}{2\pi} \int B_z d^2x$$
$$=\; \frac{1}{2\pi} \int \mathbf{rot} \, \mathbf{A} \, d^2x \;=\; \frac{1}{2\pi} \oint \mathbf{A} d\mathbf{l}. \tag{15}$$

Using a relativistic notation, which is of course the natural choice in a context of a problem involving classical electrodynamics, we rewrite this as

$$j^0 \;=\; \frac{1}{2\pi} F^{12}$$
$$=\; \frac{1}{2\pi} (\partial^1 A^2 - \partial^2 A^1)$$
$$=\; \frac{1}{4\pi} \varepsilon_{012} (\partial^1 A^2 - \partial^2 A^1), \tag{16}$$

which, taking LORENTZ invariance into account, may be generalized to

$$j^\varrho = \frac{1}{4\pi} \varepsilon_{\varrho\sigma\tau} (\partial^\sigma A^\tau - \partial^\tau A^\sigma). \tag{17}$$

Inserting this constraint into the Lagrangian we finally get

$$\begin{aligned}
L \;=\;\; & L_0 - \sum_\alpha \frac{dx_\mu^\alpha}{dt} A^\mu + \frac{1}{4\pi} \int d^2x \, \varepsilon^{\mu\nu\varrho} A_\mu \partial_\nu A_\varrho \\
=:\;\; & L_0 - \int d^2x \, j_\mu A^\mu + \frac{1}{4\pi} \int d^2x \, \varepsilon^{\mu\nu\varrho} A_\mu \partial_\nu A_\varrho \\
=:\;\; & L_0 - \left(\int d^2x \, j_\mu^{particles} - \frac{1}{4\pi} \int d^2x \, \varepsilon^{\mu\nu\varrho} \partial_\nu A_\varrho \right) A^\mu \\
=:\;\; & L_0 - \int d^2x \, (j_\mu^{particles} - j_\mu^{field}) A^\mu \\
=:\;\; & L_0 - \int d^2x \, j_\mu^{total} A^\mu.
\end{aligned} \tag{18}$$

What now seems to come as a suprise is that the quantum mechanical statistics parameter θ is exactly the fourth part of the denominator of the topological constraint term, i.e. π. This can be verified with help of functional integral techniques: Integrating out the electromagnetic vector potential A_μ we get an effective non-local action bilinear in the currents $j_\mu^{particles}$. Calculations show that a two-particle-exchange trajectory gives rise to the correct phase factor. The naive picture is consolidated if we redefine the true electric charge of the charge-flux composite as

$$Q_{true} = \int d^2x \, j_0^{total} = \int d^2x \left(j_0^{particles} - \frac{1}{4\pi} \varepsilon_{0\nu\lambda} F^{\nu\lambda} \right) = \frac{1}{2} Q, \tag{19}$$

yielding the correct statistics phase factor even in the ABAC inspired picture.[5] Thus, if the picture is true, a prerequesite for building the macroscopic Bose-condensed QHE state, is the validity of the CHERN-SIMONS dynamics, a fact emphasized by FRÖHLICH, BALACHANDRAN, and others [16, 17, 18]. Recently, GHABHOUSSI claimed the fundamental validity of the CHERN-SIMONS Lagrangian for the *integral* quantum HALL effect [18]. However, the latter is a postulate, at best comparable to the LONDON theory of superconductivity. The fundamental problem is to find a microscopic justification of this.

As early as 1984 LEVINE, LIBBY, and PRUISKEN [19] as well as PRUISKEN himself [20] decribed the integral quantum HALL effect in the language of a σ model with a topological term, in which the longitudinal and transversal components of the conductivity tensor, σ_{xx} and σ_{xy}, respectively, play the role of coupling constants. In an appropriate quantum field theoretical treatment, these are subject to renormalization expressed in terms of a two-parameter scaling analysis as shown in the pioneering work by KHMEL'NITZKII [21]. HALL conductivity plateaus correspond to vanishing CALLAN-SYMANZIK β-functions, those points, at which the quantized σ model exhibits its conformal invariance.[6] In spite of its sophistication and beauty, we think that even this model, as well as many other related approaches, are build on presuppositions, which already contain the expected result. Up to now, we have no microscopic theory of the IQHE in which the exact quantization appears as a result, not as a hidden assumption. Moreover, the debate whether the integral quantum HALL effect is a direct consequence of the fundamental laws of a dimensionally reduced quantum electrodynamics or genuinely tied to certain subtleties of semiconductor physics still seems to be open.

A theory of the quantum HALL effect should not only explain the exact quantization

---

[5]This point is missed in most popular treatments on two-dimensional statistics (e.g. anyons). The readers are often confused about the very origin of statistics transmutation. As shown, the flux-line pierced electron picture has to be supplemented by a renormalization of the effective electric charge of the composite [15].

[6]The foliated phase structure of quantum field theories with topological terms has been known for some time in the high-energy physics community, see e.g. [22, 23]. In particular, Figs. 1 and 2 of Ref. 23 anticipate the phase structure of the full quantum HALL problem ten years before it became clear [12]. One of us (R.D.T.) is indebted to R.L. STULLER for this remark.

of the transversal conductivity but also describe the exact shape of the curves, which are only step and delta functions in the limit of zero temperature. Clearly, LANDAU levels are broadened by impurity scattering, but this effect alone does not explain the shape of the longitudinal and transversal resistivity curves. For the many different approaches to the problem the reader is refered to [3,4,5,6,7].

Some time ago CHANG and TSUI [24] observed that the derivative of the finite-temperature quantum HALL resistance ϱ_{yx} with respect to the two-dimensional carrier density n_{2D} exhibits a remarkable similarity to the longitudinal resistivity ϱ_{xx} to the extent that one is almost directly proportional to the other, i.e.

$$\frac{d\varrho_{yx}}{dn_{2D}} \approx -a \cdot \varrho_{xx}. \tag{20}$$

Two significant deviations of this behaviour should be mentioned: Firstly, the relation does no longer hold in the classical regime $B \to 0$ and, secondly, the spikes appearing in the derivative of the transversal resistivity are smeared out in the longitudinal one.

What is the reason for this apparently fundamental relation between the two quantities? CHANG and TSUI speculate about a KRAMERS-KRÖNIG type relation based on causality [25]. The presence of a natural frequency scale ω_c, the cyclotron frequency, and the suggestive association of the longitudinal and transversal resistivities as parts of a generalized complex resistivity describing a general type of a dielectric response phenomenon in the sense of KELDYSH et al. [26] should give rise to this kind of dispersion relation. We cannot expect, however, that the standard KUBO formula treatment does provide a background for this speculation as claimed by CHANG and TSUI in their 1985 paper [24] since it certainly does not contain all the information necessary for a thorough treatment of the electromagnetic response problem defined by the quantum HALL setup [27].

The relation discovered by CHANG and TSUI can only directly verified in gated systems where we can continuously control the two-dimensional charge carrier density n_{2D}. Therefore, in the context of this paper, it is interesting to reexpress the derivative relation in terms of the resistivities and the magnetic field alone. If one assumes that the filling factor

$$\nu = \frac{n_{2D}h}{eB} \tag{21}$$

is the relevant variable, we may write

$$\frac{d\varrho_{yx}}{dn} = \frac{d\varrho_{yx}}{d\nu}\frac{d\nu}{dn_{2D}} = \frac{d\varrho_{yx}}{dB}\frac{dB}{d\nu}\frac{d\nu}{dn_{2D}} = -\frac{1}{n_{2D}}\frac{d\varrho_{yx}}{dB}\cdot B. \tag{22}$$

Combining both equations we obtain

$$\frac{d\varrho_{yx}}{dB} \approx a \cdot \frac{n_{2D}}{B} \cdot \varrho_{xx}. \tag{23}$$

Within a simple scaling model VAGNER and PEPPER discuss some generalizations of this formula [28]. Assumptions on the nature of the impurity scattering, on the spatial variations of the transversal resistivities, on the strength of the applied magnetic field etc. restrict the possible values of the exponents of the general, still phenomenological, formula

$$\frac{d\varrho_{yx}}{dB} \approx a \cdot n_{2D} \cdot B^s \cdot \varrho_{xx}^t. \tag{24}$$

In the cases accessible in our experiments we have $t = 1$ with s being a small positive or negative number of order 10^{-2} for a negative or positive slope of $\varrho_{xx}(B)$ at $B = 0$, respectively.

We will use these phenomenological formulas as a basis of numerical simulations where we average over a finite number of replicas with a certain distribution of values simulating inhomogenities of the two-dimensional charge carrier density n_{2D} and external magnetic field B.

Our stategy is to push quantum HALL experiments to the extremes - in a truly literal sense! If this effect is really a macroscopic quantum effect, then it should be as robust as superconductivity, where it is possible to create situations where the macroscopic quantum state is extended over a region of many kilometers. Furthermore such a state should exhibit a robustness which allows a "quick 'n' dirty" preparation. Nevertheless it still should exhibit features uniquely associated with the topology of boundary conditions. This paper is intended to be a first step toward a realization of this strategy, following a (more or less) crazy suggestion by one of us (A.D.W.) to Professor VON KLITZING some time ago, namely to investigate the quantized HALL effects on huge samples [29].

To summarize, there are three main reasons to do so:

1. To study the general limits of *macroscopic* quantum coherence attributed to the quantum HALL phenomenon.

2. To study the scaling laws in the *infrared* (using the terminology of quantum field theory), i.e. in the large scale regime.

3. To study the influence of inhomogenities of the charge carrier density, the mobility, and the external magnetic field on the *"spectral smearing"* of the QHE signal.

The latter topic seems to be of great importance in quality control management of III-V (GaAs) molecular beam epitaxy (MBE); for a review on this topic see [30]. If it is possible to interpret a huge sample quantum HALL curve in an appropriate way we will have a technique to measure the quality, say *electrical* homogenity, of a full wafer in a purely electronic, non-destructible way.

The remaining part of the paper is organized as follows: In the next section we present some computer simulations based on a simple phenomenological model. This enables us to get a feeling about the influence of inhomogenities on the shape of the quantum HALL curve. In what follows we briefly describe the experimental set-up including the preparation of the samples. Finally, we review the experimental results, try to interpret them, and make some suggestions towards future research.

2   Computer simulations

The classical formula for the HALL resistance in case of a HALL bar geometry is given by

$$R_H^{cl} = \frac{B}{en_{2D}} = \frac{h}{\left(\dfrac{hn_{2D}}{eB}\right)e^2} \ . \tag{25}$$

The quantum analog reads

$$R_H^{qu} = \frac{h}{\nu e^2}. \tag{26}$$

Consequently, an idealized quantum HALL curve, in which the HALL resistance $R_H^{ideal}(B)$ is understood as a function depending on the external magnetic field B is given by the assignment

$$\nu \longmapsto \nu(B) = \begin{cases} \text{int}\left(\dfrac{hn_{2D}}{eB} + \dfrac{1}{2}\right) & \text{if} & \dfrac{hn_{2D}}{eB} > \dfrac{1}{2} \\ \dfrac{hn_{2D}}{eB} & \text{else} \end{cases} \tag{27}$$

The "else" condition guarantees that below $\nu = 1$ the curve is classical as will be expected if the fractional effect is absent. The case including spin degeneracy is modelled in an analogous way (Figures 1-4).

Averaging may be done additively (arithmetic mean), multiplicatively (geometric mean), or reciprocal additively (harmonic mean) by scattering the parameters for the two-dimensional charge carrier density and the external magnetic field around selected fixed values. In case of a different geometry than the HALL bar one an additional multiplicative factor γ has to be included

$$R_H^{cl} = \frac{\gamma B}{en_{2D}} = \frac{h}{\left(\dfrac{hn_{2D}}{e\gamma B}\right)e^2} \tag{28}$$

in such a way that the quantization (which must not depend on geometry) stays intact:

$$R_H^{qu} = \frac{h}{\nu e^2}. \tag{29}$$

Geometry factors may vary as well and can be absorbed in a redefinition of the two-dimensional carrier density and magnetic field, respectively, introducing new effective quantities n_{2D}^{eff} and B^{eff}. This may be useful in comparing totally different kinds of specimens.

The mathematically inequivalent averaging methods correspond to different quantum HALL-sample-network models such as arrangements in series, parallel, or combinations thereof. However, in cases of a sufficiently narrow distribution of values ($\leq 6\%$) it does not matter which method we prefer since then the results of all averaging methods nearly coincide.

Including in this algorithm the proposal by VAGNER and PEPPER [28] we get a fairly good simulation of realistic HALL curves which explicitely show up the smoothing of the steps and exhibit an extremely realistic behaviour of the logitudinal resistance. This can be seen in Figures 5-10. Clearly, our averaging model does not include microscopic mechanisms such as quantum interference. However, our diagrams can be used as a reference in the study of experimental curves to get knowledge about the large scale behaviour.

3   Experiments with topological trivial samples

We grow a $GaAs/Al_{0.33}Ga_{0.67}As$ modulation doped heterostructure by molecular beam epitaxy on a semi-insulating GaAs (100) substrate. It consists of a 2 μm nominally doped GaAs buffer layer and a 23 nm undoped $Al_{0.33}Ga_{0.67}As$ spacer layer, followed by 50 nm of Si doped $Al_{0.33}Ga_{0.67}As$ and a 10 nm GaAs cap. The two-dimensional electron gas is localized in a sheet within the GaAs buffer right at the interface to the spacer.

The measured values for the electron sheet density and the electron mobility are

- at room temperature 3.36×10^{11} cm^{-2} and $6\,477$ cm^2 V^{-1}s^{-1}

- at T=77 K in the dark 3.33×10^{11} cm^{-2} and $84\,600$ cm^2 V^{-1}s^{-1}

- at T=5 K in the dark 3.1×10^{11} cm^{-2} and $336\,000$ cm^2 V^{-1}s^{-1}

After the growth process the wafer (#7235) is cut into parts. One sample is mesa-etched into a standard HALL-bar geometry with a width of 150 μm and a distance of 200 μm between ohmic contacts which were made with an AuGe/Ni alloy. Thus in this type of specimen (called "**micro**") we have an electric active area of some 0.1 mm^2 depending on the patching. The other ones are square-shaped VAN DER PAUW-type [31] specimens of 3×3 mm^2 = 9 mm^2 (called "**milli**") of 1.5 cm $\times 1.5$ cm = 625 mm^2 (called "**centi**"), respectively. Roughly speaking, this collection of samples enables us to study real-space scaling experimentally over four orders of magnitude, which is a lot! (The next two orders of magnitude would require specimens of about $100\,000$ mm^2 corresponding to full 300 mm wafers, which are not available yet.) The larger specimens were contacted "quick 'n' dirty" by alloying-in some indium at the corners and the inner edges, respectively. This was done under an nitrogen-hydrogen atmosphere. The samples are mounted on a chip carrier and the measurement was done in a standard way using a home-made[7] metal cryostat used in experimental lab courses. The arrangements of the contacts and the sample geometry are shown in Figures 11-16.

Experimental results are shown in Figures 17-27 and Tables 1-3. We observed an interesting aging effect, a drop of the signal for the longitudinal resistivity which disappeared

---

[7]by one of us (A.D.W.)

after an experimental rest (Figures 17-22). The effect could be reproduced and was probably attributed to the thermodynamics of the set-up, which eventually caused one sample to break (see Figure 14).

As a main result of our investigations, the scaling behaviour can be read off from Figures 23-25 and, finally, from Figure 26 and Table 1.

In the literature, scaling mostly is discussed not by considering the renormalization of the sample size in real space but, rather, in terms of its low temperature behaviour. Essentially, the dependence of conductance on temperature is equivalent to its dependence on the sample size. In a very interesting experiment H.-P. WEI *et al.* performed such a scaling analysis for the quantum HALL problem [33, 34]. Essentially, they observed the behaviour of the derivative of the transversal HALL resistance with respect to the temperature, which diverges algebraically with $T \to 0$. For the critical exponent which characterizes this divergence they obtain from measurements between 4.2 and 0.1 K a universal value of 0.42.

In any finite-temperature experiment an effective sample size is determined by the THOULESS length which is a measure of the mean free path for inelastic scattering. But the temperature-size analogy rests on certain assumptions which may be questioned in the very large scale limit, such that, of course, it makes sense to perform a real-space experiment in the laboratory. By rescaling the magnetic field the curves in Figure 26 are normalized in such a way that they can be compared directly. In Table 1 we list some characteristic properties of the curves, from which the reader may find an appropriate phenomenological formula. In terms of our numerical simulations the samples corresponds to a family of replica of an idealized reference sample with a variation of parameters (i.e. the plateau width) within a few percent range showing again the robustness of the effect.

Two qualitative observations should be underlined: Firstly, whereas the higher plateaux ($\nu > 4$) are smeared out, the lower seems to become more pronounced and stable for very large samples, secondly, the lifting of the spin degeneracy is worse for huge specimens. That is probably due to the fact that polarized domains have an characteristic maximum size.

Of course, our samples are not ideal. But, in general, it is very difficult to distinguish between genuine effects and effects attributed to additional imperfections introduced

by the specific production process which may be afflicted with one or another shortcoming in the MBE growth. According to common wisdom the quantum HALL effect is a localization-delocalization phenomenon due to a mild form of disorder and therefore it is almost impossible to define an idealized reference sample. Nevertheless it would be useful to do this empirically by repeating these experiments again and again and logging them.

4   Measurements on topological non-trivial samples

Like the setup proposed by VAN DER PAUW [31] the technique utilizing a CORBINO disk (i.e. a ring shaped sample) can be used to measure HALL mobilities in different types of semiconductors, see e.g. [35], or the low-temperature parameters of a two-dimensional electron gas [36].

In the study of the *quantized* HALL effect the CORBINO technique enables us to study situations in which the samples are contactless (with respect to the injected current) and hence the currents are edgeless. This is interesting since it provides us with information on the physics in the bulk. The connection between 2+1 dimensional CHERN-SIMONS quantum field theory and 1+1 dimensional conformal field theory indicate, from first principles of quantum physics and gauge theory alone, that the edge and the bulk pictures should not be seen as concurrent but rather as complementary and, hence, compatible approaches, e.g. [37, 38]. Thus the analysis of the CORBINO topology definitely completes our understanding of a two-dimensional quantum-electrodynamical response phenomenon.

In the edgeless case current is induced inductively either by modulating the external magnetic field with an a.c. driven solenoid [39, 40, 41] or by a capacitive coupling [42, 43]. The independent injection of different currents into the different connected components of the topologically disconnected boundary in a ring geometry was also studied [44]. WOLF *et al.* produced window-shaped quantum HALL effect samples with contacts both on the inner and on the outer edges. This allowed them to study potentials appearing on contacts inside a sample but still lying on an edge and hence not decoupling from the two-dimensional electron gas [45]. Their experimental results indicate that under quantum HALL effect conditions there is no electron transfer between the inner and the outer edge.

In our experiments we performed conventional quantum HALL measurements on a very large VAN DER PAUW-CORBINO hybrid geometry/topology. The sample is a square shaped device of 1.5 cm^2 × 1.5 cm^2 with a centered hole of 7 mm diameter. The latter was milled out by putting the varnished specimen in a spinner and applying a pen-like rod of wood with sandpaper glued on its bottom. (As a rather unconventional method it is without any respect.) Contacts were soldered in exact the same way as in the case of the samples with trivial topology. Experimental results are shown in Figure 27 and commented in Table 3.

Whereas it is interesting in itself that even in the topological non-trivial case everything works fine with this "quick 'n' dirty" preparation we should point the reader onto two interesting additional observations: Firstly, the behavior of the slopes in the longitudinal resistivity depending on the fact whether it is measured inside or outside (curves γ and δ) and, secondly, the onset of a second-derivative content if the current is injected on the different boundary than on which the voltage is measured (curve ζ). However, these structures are not always as pronounced and vary.

5   Conclusion

From the viewpoint of a professional technician our experiments may look a little bit sportive if not amateurish. However, from the viewpoint of a theoretician who is interested in first principles our investigations definitely have the flavour of *realized* gedankenexperiments intimately touching the first principles underlying our field of interest, namely the mesoscopic realization of a dimensionally reduced 2+1 dimensional quantum electrodynamics.

The main result of our work is: Yes, the integral quantum HALL effect is indeed a *macroscopic*, extremely robust, quantum phenomenon.

How far can we go? Clearly, one should repeat all measurements on still larger samples (up to 300 mm wafers, if they are available, placed in high-energy accelerator detector magnets), at lower temperatures (down to mK range) and on samples of higher genera in the language of analytic function theory (i.e. with more holes). Of course, it would be useful to study the scaling laws in more detail experimentally although the essence is

already captured in Figure 26 and Table 1.

If we add techniques like focused ion beam lithography, in particular in-plane gated set-ups [46, 47] we probably could observe the topological transition from a Corbino disk to a Hall bar or from a Corbino to a van der Pauw geometry. In other words, we could perform experiments within a unique topology changing scenario in mesoscopic physics, as it was recently done with help of different preparation methods [48]. Last but not least we should mention the famous fountain pressure experiments by Klass *et al.* which could give us additional relevant information about the physics in these huge samples [49].

6   Acknowledgements

7   References

[1] K. VON KLITZING, G. DORDA, and M. PEPPER, *New method for high-accuracy determination of the fine-structure constant based on quantized Hall resistance*, Phys. Rev. Lett. **45**, 494-497 (1980)

[2] P.A.M. DIRAC, *Quantized singularities in the electromagnetic field*, Proc. Roy. Soc. **A133**, 60-72 (1931)

[3] R.E. PRANGE and S.M. GIRVIN, *The Quantum Hall Effect*, Springer-Verlag, Berlin 1987

[4] M. STONE ed., *Quantum Hall Effect*, World Scientific, Singapore 1992

[5] M. JANSSEN, O. VIEHWEGER, U. FASTENRATH, and J. HAJDU, *Introduction to the Theory of the Integer Quantum Hall Effect*, Verlag Chemie, Weinheim 1994

[6] T. CHAKRABORTY and P. PIETILÄINEN, *The Quantum Hall Effects*, Springer-Verlag, Berlin 1995

[7] K. EFETOV, *Supersymmetry in Disorder and Chaos*, Cambridge University Press 1997

[8] F.D.M. HALDANE and L. CHEN, *Magnetic flux of "vortices" on the two-dimensional Hall surface*, Phys. Rev. Lett. **53**, 2591 (1984)

[9] J.K. JAIN, *Theory of the fractional quantum Hall effect*, Phys. Rev. **B41**, 7653-7665 (1990)

[10] S.-C. ZHANG, T.H. HANSON, and S. KIVELSON, *Effective-field-theory model for the fractional quantum Hall effect*, Phys. Rev. Lett. **62**, 82-85 (1989)

[11] S.-C. ZHANG, *The Chern-Simons-Landau-Ginzburg theory of the fractional quantum Hall effect*, Int. J. Mod. Phys. B6, 25-58 (1992)

[12] S. KIVELSON, D.-H. LEE, and S.-C. ZHANG, *Global phase diagramm in the quantum Hall effect*, Phys. Rev. **B46**, 2223-2238 (1992)

[13] Y. AHARONOV and D. BOHM, *Significance of electromagnetic potentials in the quantum theory*, Phys. Rev. **115**, 485-491 (1959)

[14] Y. AHARONOV and A. CASHER, *Topological quantum effects for neutral particles*, Phys. Rev. Lett. **53**, 319-321 (1984)

[15] X.G. WEN and A. ZEE, *On the possibility of a statistics-changing phase transition*, J. Phys. France **50**, 1623-1629 (1989)

[16] J. FRÖHLICH and A. ZEE, *Large scale physics of the quantum Hall fluid*, Nucl. Phys. **B364**, 517-540 (1991)

[17] A.P. BALACHANDRAN, *Chern-Simons dynamics and the quantum Hall effect*, Preprint Syracuse SU-4228-492 (1991). Published in a volume in honor of Professor R. Vijayaraghavan.

[18] F. GHABOUSSI, *Quantum theory of the Hall effect*, Int. J. Theor. Phys. **36**, 923-934 (1997)

[19] H. LEVINE, S.B. LIBBY, and A.M.M. PRUISKEN, *Theory of the quantized Hall effect I*, Nucl. Phys. **B240** (FS12), 30-48 (1984); *II*, Nucl. Phys. **B240** (FS12), 49-70 (1984); *III*, Nucl. Phys. **B240** (FS12), 71-90 (1984)

[20] A.M.M. PRUISKEN, *On localization in the theory of the quantized Hall effect: a two dimensional realization of the theta vacuum*, Nucl. Phys. **B235** (FS11), 277-298 (1984)

[21] D.E. KHMEL'NITZKII, *Quantization of Hall conductivity*, JETP Lett. **38**, 552-556 (1983)

[22] J.L. CARDY and E. RABINOVICI, *Phase structure of Z(P) models in the presence of a theta parameter*, Nucl. Phys. **B205** (FS5) 1-16 (1982)

[23] J.L. CARDY and E. RABINOVICI, *Duality and the theta parameter in abelian lattice models*, Nucl. Phys. **B205** (FS5) 17-26 (1982)

[24] A.M. CHANG and D.C. TSUI, *Experimental observation of a striking similarity between quantum Hall transport coefficients*, Solid State Comm. **56**, 153-154 (1985)

[25] G.D. MAHAN, *Many-Particle Physics*, Plenum Press, New York 1986

[26] L.V. KELDYSH, D.A. KIRZHNITZ, and A.A. MARADUDUIN, *The dielectric function of condensed systems*, North-Holland, Amsterdam 1989

[27] N. SCHOPOHL, private communication.

[28] I.D. VAGNER and M. PEPPER, *Similarity between quantum Hall transport coefficients*, Phys. Rev. **37**, 7147-7148 (1988)

[29] K. VON KLITZING, private communication.

[30] M.A. HERMANN and H. SITTER, *Molecular Beam Epitaxy*, Springer-Verlag, Berlin (1989)

[31] L.J. VAN DER PAUW, *A method of measuring specific resistivity and Hall effects of discs of arbitrary shape*, Philips Research Reports **13**, 1-9 (1958)

[32] M.A. HERMANN and H. SITTER, *Molecular Beam Epitaxy*, Springer-Verlag, Berlin (1989)

[33] H.P. WEI, D.C. TSUI, M.A. PAALANEN, and A.M.M. PRUISKEN, *Experiments on delocalization and universality in the integral quantum Hall effect*, Phys. Rev. Lett. **61**, 1294-1296 (1988)

[34] H.P. WEI, S.Y. LIN, D.C. TSUI, and A.M.M. PRUISKEN, *Effect of long-range potential fluctuations on scaling in the integer quantum Hall effect*, Phys. Rev. **45**, 3926-3928 (1992)

[35] G.P. CARVER, *A Corbino disk apparatus to measure Hall mobilities in amorphous semiconductors*, Rev. Scient. Instr. **43**, 1257-1263 (1972)

[36] I.M. TEMPLETON, *A simple contactless method for evaluating the low-temperature parameters of a two-dimensional electron gas*, J. Appl. Phys. **62**, 4005-4007 (1987)

[37] A.P. BALACHANDRAN, L. CHANDAR, and B. SATHIAPALAN, *Duality and the fractional quantum Hall effect*, Nucl. Phys. **B443**, 465-500 (1995)

[38] A.P. BALACHANDRAN, L. CHANDAR, and B. SATHIAPALAN, *Chern-Simons duality and the fractional quantum Hall effect*, Int. J. Mod. Phys. **A11**, 3587-3608 (1996)

[39] P.F. FONTEIN, J.M. LAGEMAAT, J. WOLTER, and J.P. ANDRE, *Magnetic field modulation - a method for measuring the Hall conductance with a Corbino disc*, Semiconductor Science and Technology **3**, 915-918 (1988)

[40] B. JEANNERET, B.D. HALL, H.-J. BUHLMANN, R. HOUDRE, M. ILEGEMS, B. JECKELMANN, and U. FELLER, *Observation of the integer quantum Hall effect by magnetic coupling to a Corbino ring*, Phys. Rev. **B51**, 9752-9756 (1995)

[41] B. JEANNERET, B.D. HALL, B. JECKELMANN, U. FELLER, H.-J. BUHLMANN, and M. ILEGEMS, *AC measurements of edgeless currents in a Corbino ring in the quantum Hall regime*, Solid State Comm. **102**, 287-290 (1997)

[42] C.L. PETERSEN and O.P. HANSEN, *Two-dimensional electron gases in the quantum Hall regime: analysis of the circulating current in contactless Corbino geometry*, Solid State Comm. **98**, 947-950 (1996)

[43] C.L. PETERSEN and O.P. HANSEN, *The diagonal and off-diagonal AC conductivity of two-dimensional electron gases with contactless Corbino geometry in the quantum Hall regime*, J. Appl. Phys. **80**, 4479-4483 (1996)

[44] R.G. MANI, *Steady-state bulk current at high magnetic fields in Corbino-type GaAs/AlGaAs heterostructure devices*, Europhys. Lett. **36**, 203-208 (1996)

[45] H. WOLF, G. HEIN, L. BLIEK, G. WEIMANN, and W. SCHLAPP, *Quantum Hall effect in devices with an inner boundary*, Semiconductor Science and Technology **5**, 1046-50 (1990)

[46] R.J. HAUG, A.D. WIECK, and K. VON KLITZING, *Magnetotransport properties of Hall-bar with focused-ion-beam written in-plane-gate*, Physica **B184**, 192-196 (1993)

[47] R.D. TSCHEUSCHNER and A.D. WIECK, *Quantum ballistic transport in in-plane-gate transistors showing onset of a novel ferromagnetic phase transition*, Superlattices and Microstructures **20**, 616-622 (1996)

[48] A.S. SACHRAJDA, Y. FENG, R.P. TAYLOR, R. NEWBURY, P.T. COLERIDGE, J.P. MCCAFFREY, *The topological transition from a Corbino to Hall bar geometry*, Superlattices and Microstructures **20**, 651-656 (1996)

[49] U. KLASS, W. DIETSCHE, K. VON KLITZING, and K. PLOOG, *Fountain-pressure imaging of the dissipation in quantum-Hall experiments*, Physica **B169**, 363-367 (1991)

8   Figures: Numerical simulations
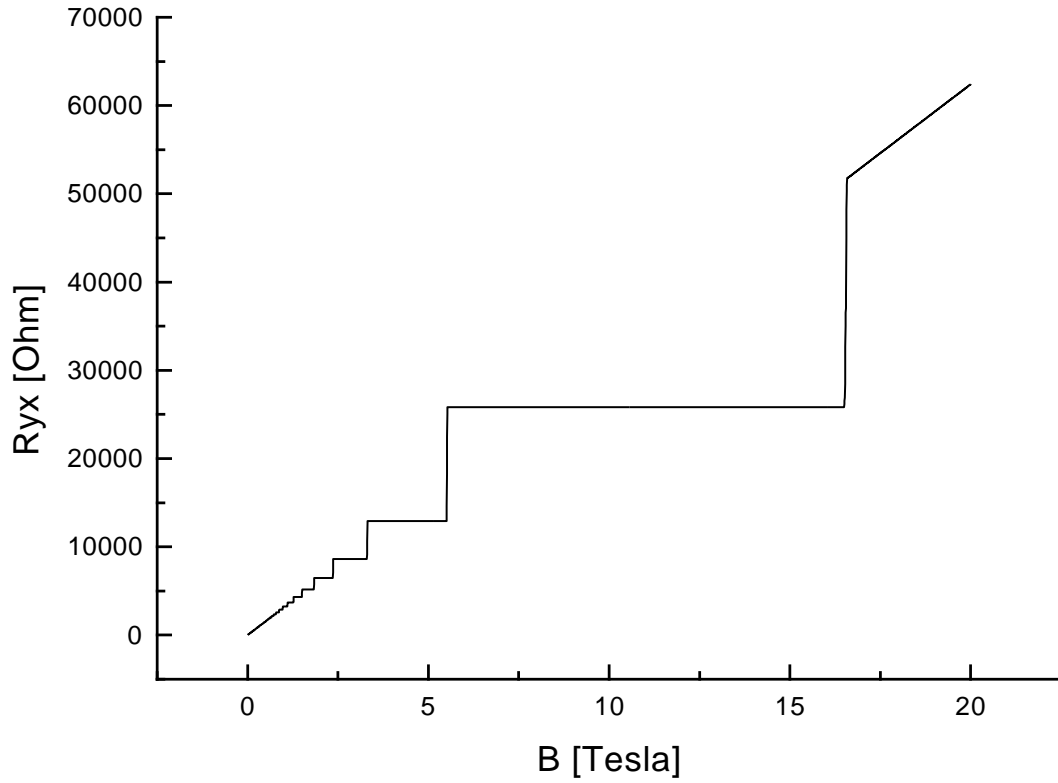
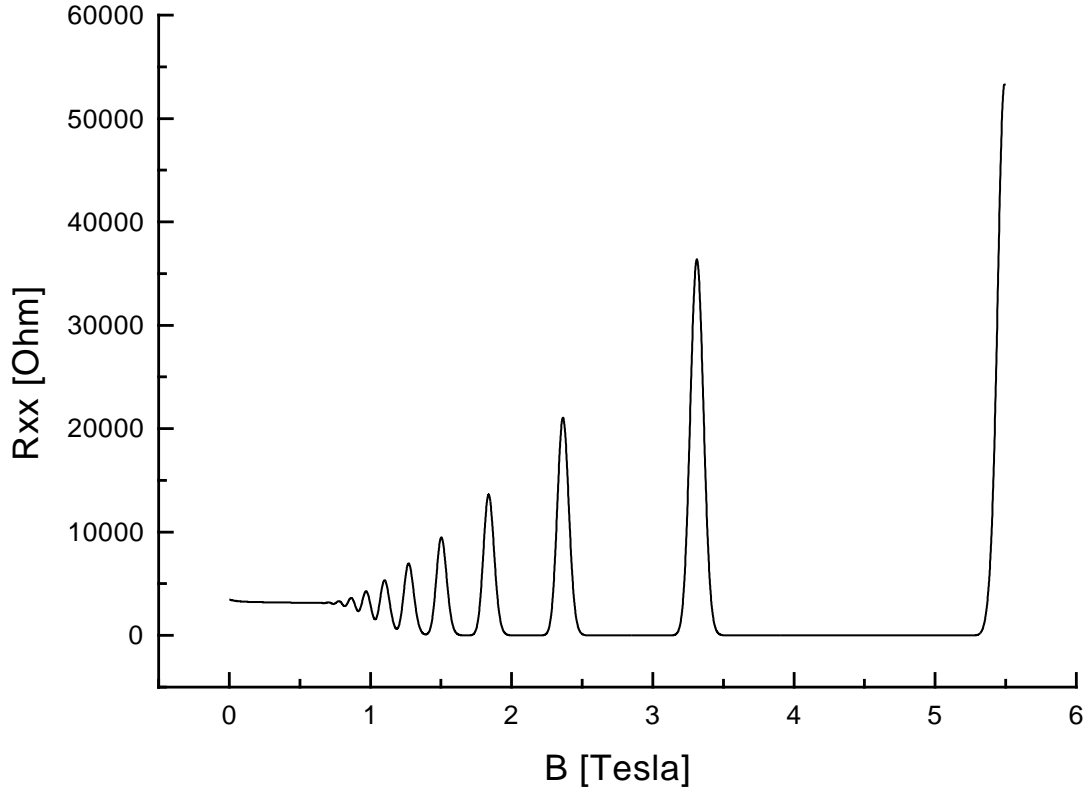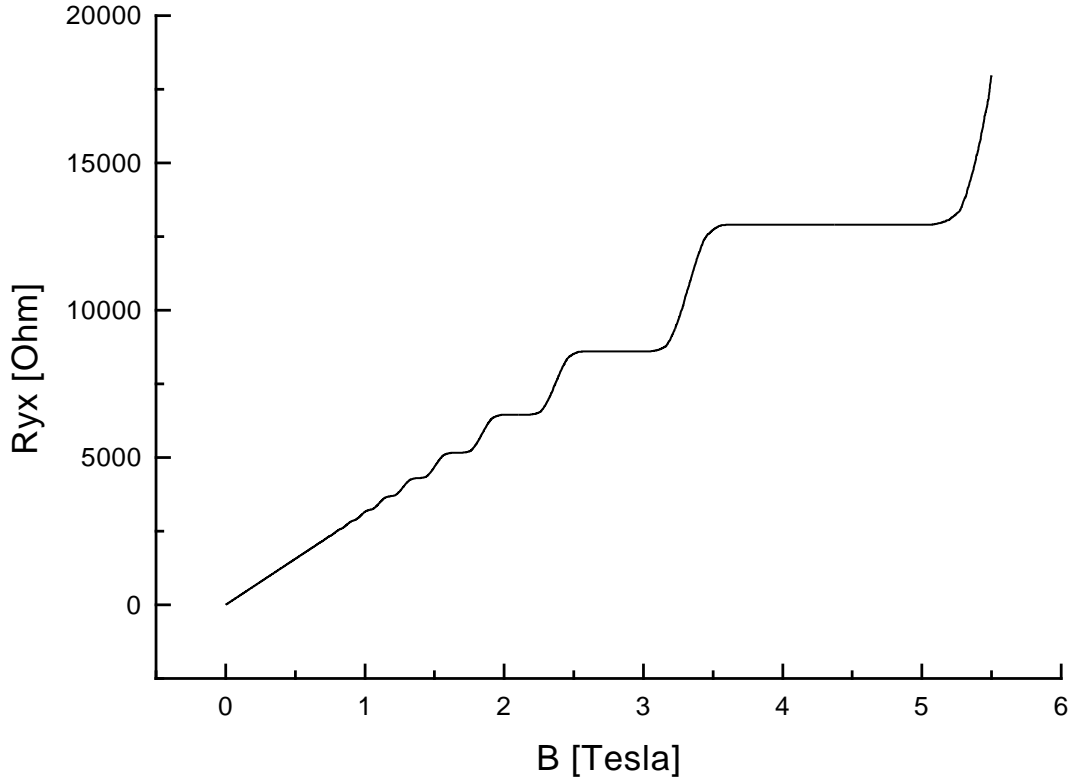Figure 1: Nearly ideal *transversal* quantized HALL resistance (without spin degeneracy) down to filling factor $\nu = 1$. (Computer simulation based on a phenomenological formula averaging over $N > 50$ replicas within a charge carrier density variance $\sigma < 0.1\,\%$ around $n_{2D} \approx 2.0 \cdot 10^{15}/\mathrm{m}^2$.)
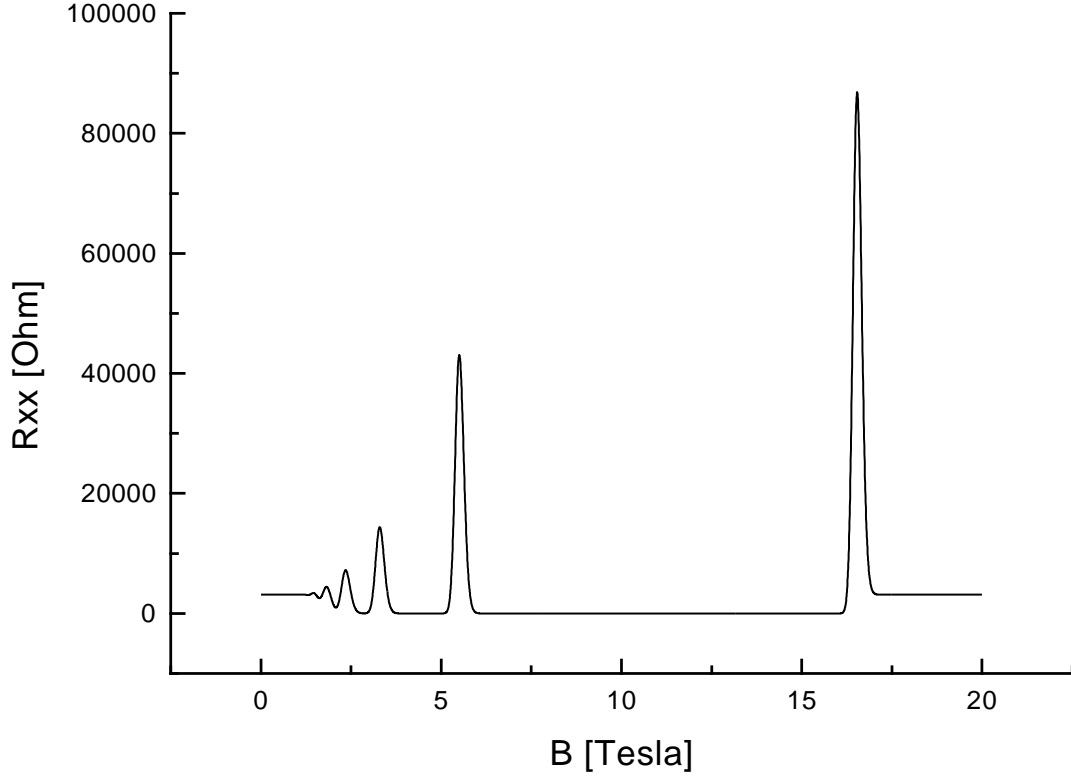
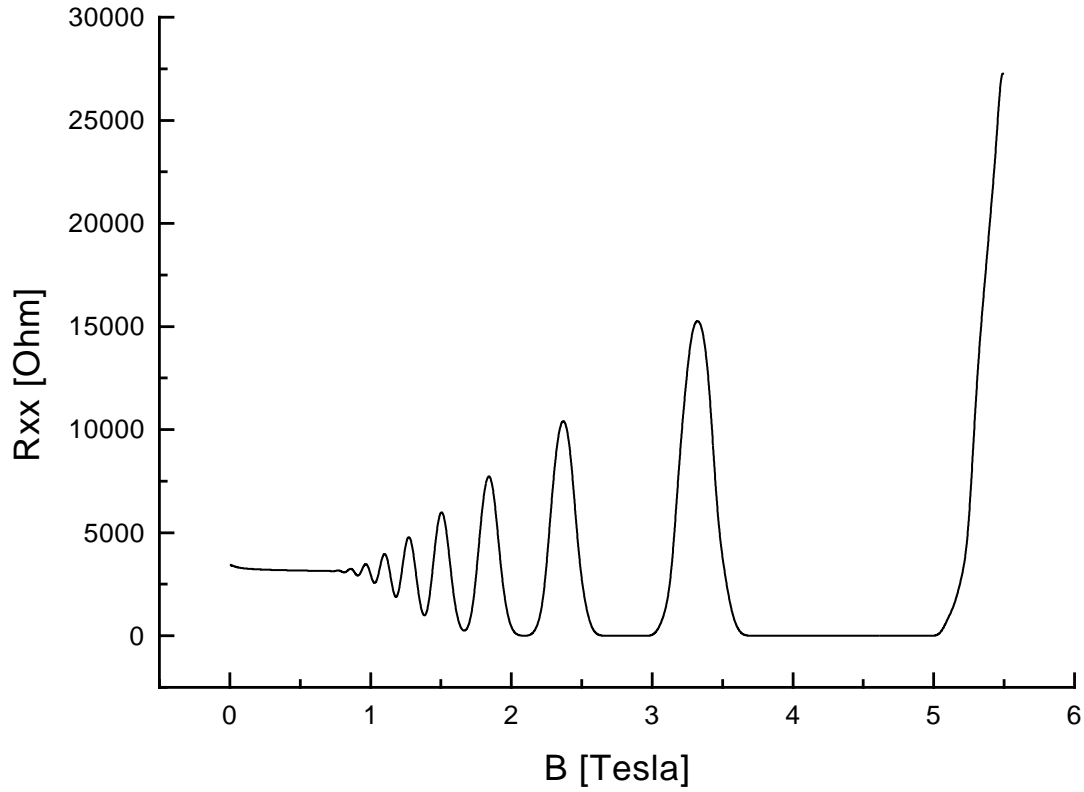Figure 2: Nearly ideal *longitudinal* quantized HALL resistance (without spin degeneracy) down to filling factor $\nu = 1$. (Computer simulation based on a phenomenological formula averaging over $N > 50$ replicas within a charge carrier density variance $\sigma < 0.1\,\%$ around $n_{2D} \approx 2.0 \cdot 10^{15}/\mathrm{m}^2$.)
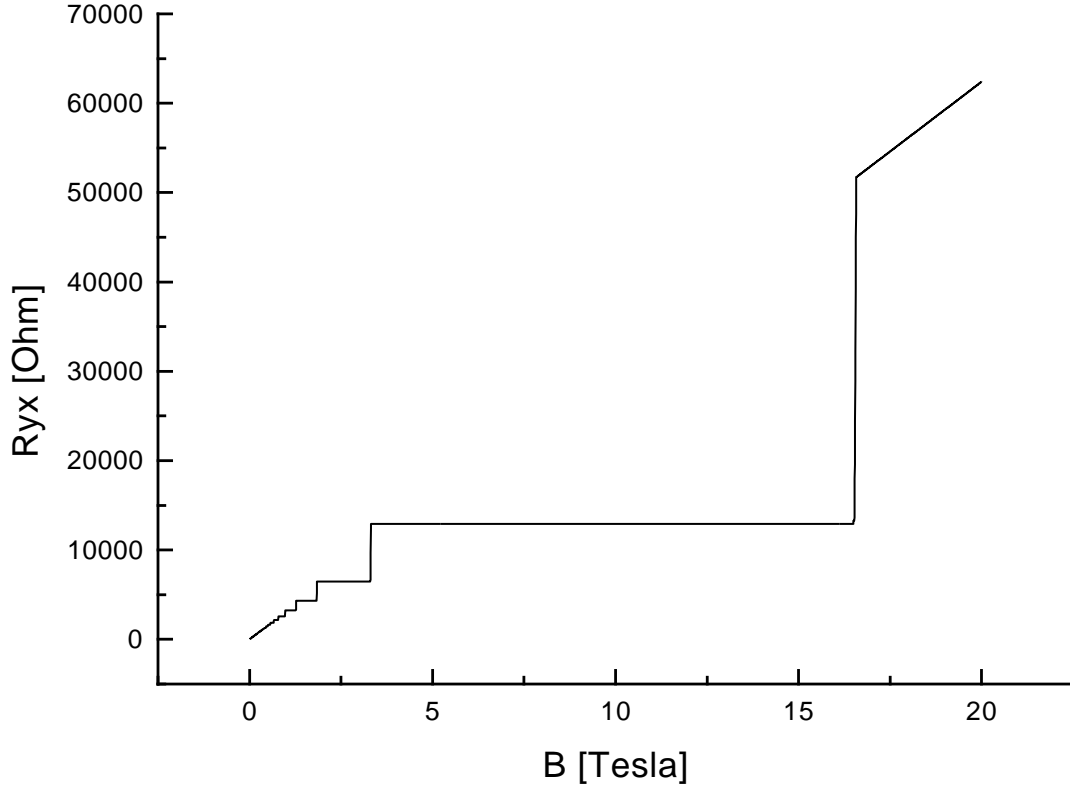
Figure 3: Nearly ideal *transversal* quantized HALL resistance *including* spin degeneracy down to filling factor $\nu = 2$. (Computer simulation based on a phenomenological formula averaging over $N > 50$ replicas within a charge carrier density variance $\sigma < 0.1\%$ around $n_{2D} \approx 2.0 \cdot 10^{15}/\text{m}^2$.)
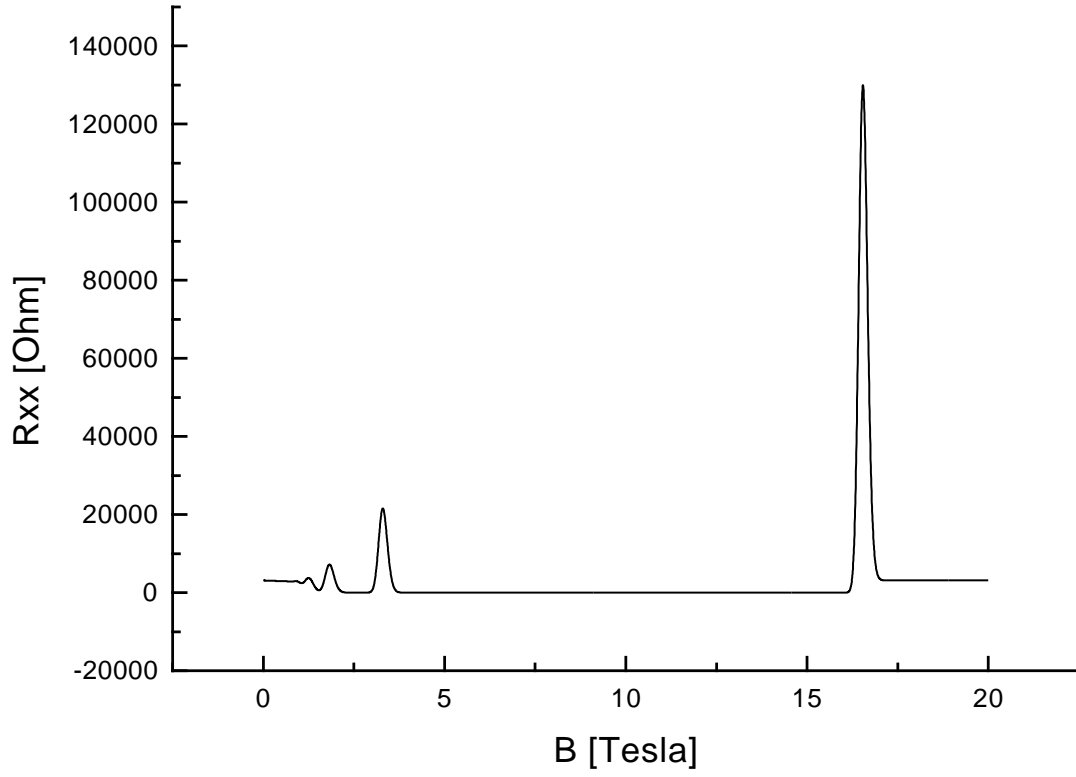
Figure 4: Nearly ideal *longitudinal* quantized HALL resistance *including* spin degeneracy down to filling factor $\nu = 2$. (Computer simulation based on a phenomenological formula averaging over $N > 50$ replicas within a charge carrier density variance $\sigma < 0.1\,\%$ around $n_{2D} \approx 2.0 \cdot 10^{15}/\mathrm{m}^2$.)
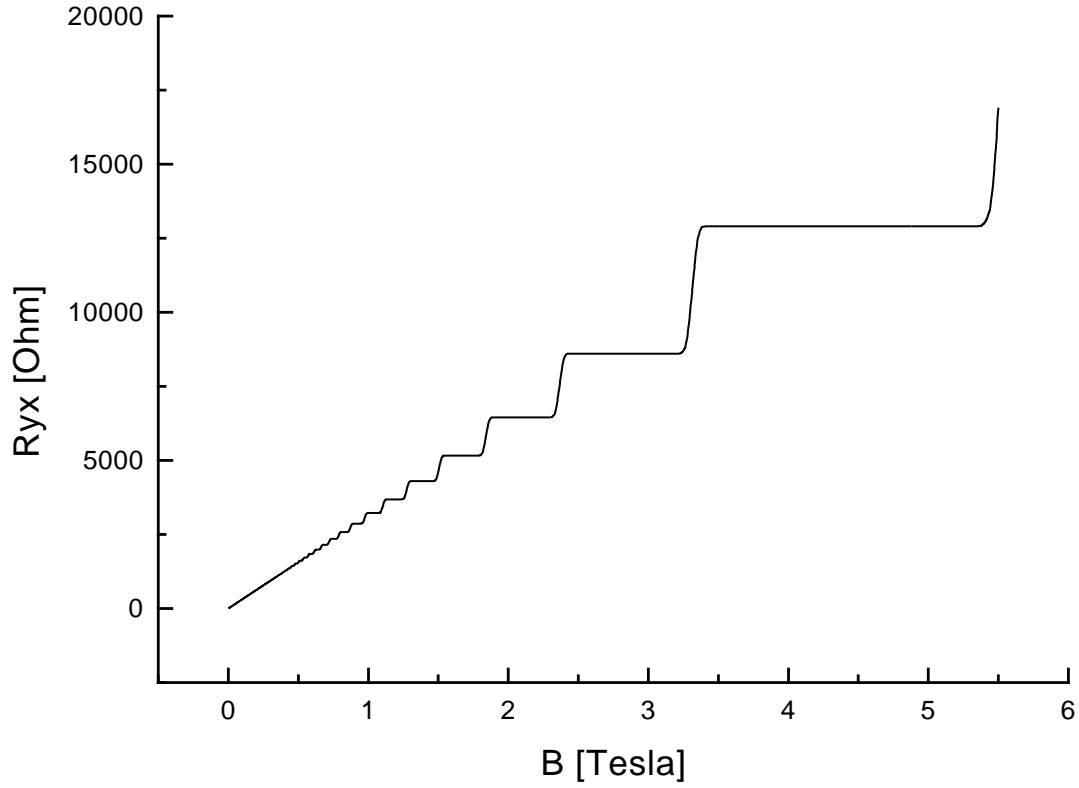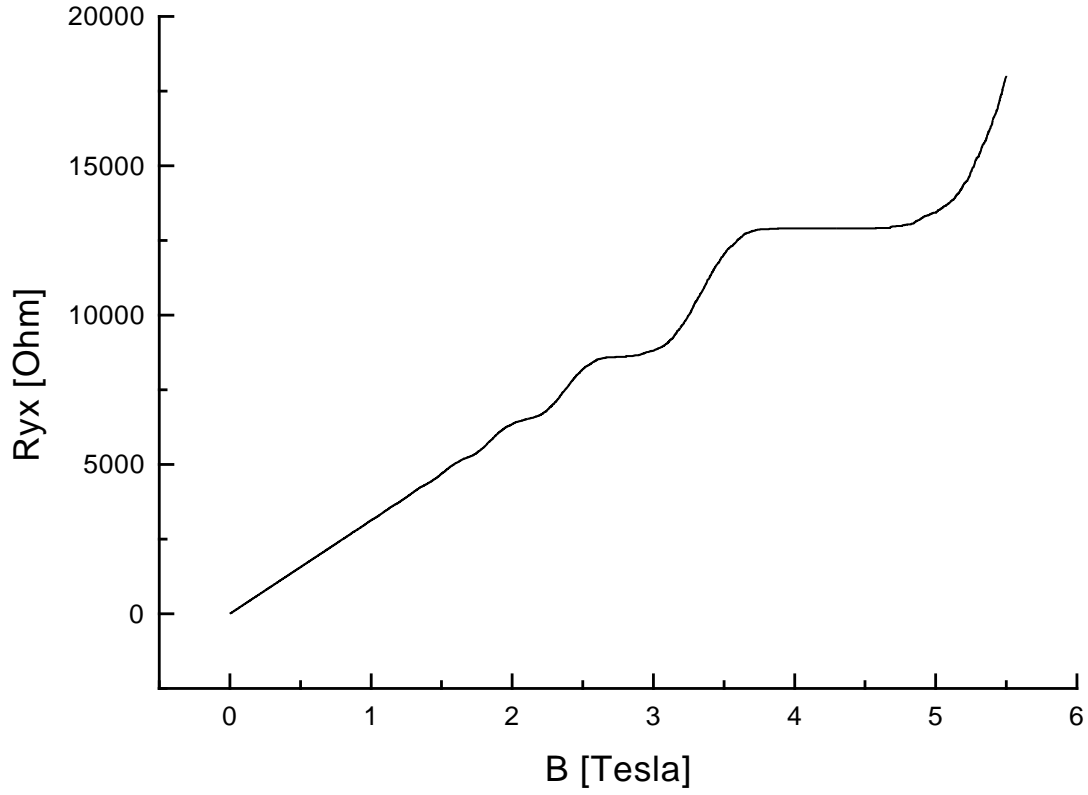
Figure 5: *Transversal* quantized HALL resistance (without spin degeneracy) down to filling factor $\nu = 1$. (Computer simulation based on a phenomenological formula *geometrically* averaging over $N = 1000$ replicas within a charge carrier density variance $\sigma = 1\,\%$ around $n_{2D} \approx 2.0 \cdot 10^{15}/\mathrm{m}^2$. Inhomogenities of the external magnetic field may be modelled in an analogous fashion.)

Figure 6: *Longitudinal* quantized HALL resistance (without spin degeneracy) down to filling factor $\nu = 1$. (Computer simulation based on a phenomenological formula *geometrically* averaging over $N = 1000$ replicas within a charge carrier density variance $\sigma = 1\%$ around $n_{2D} \approx 2.0 \cdot 10^{15}/\text{m}^2$. Inhomogenities of the external magnetic field may be modelled in an analogous fashion.)
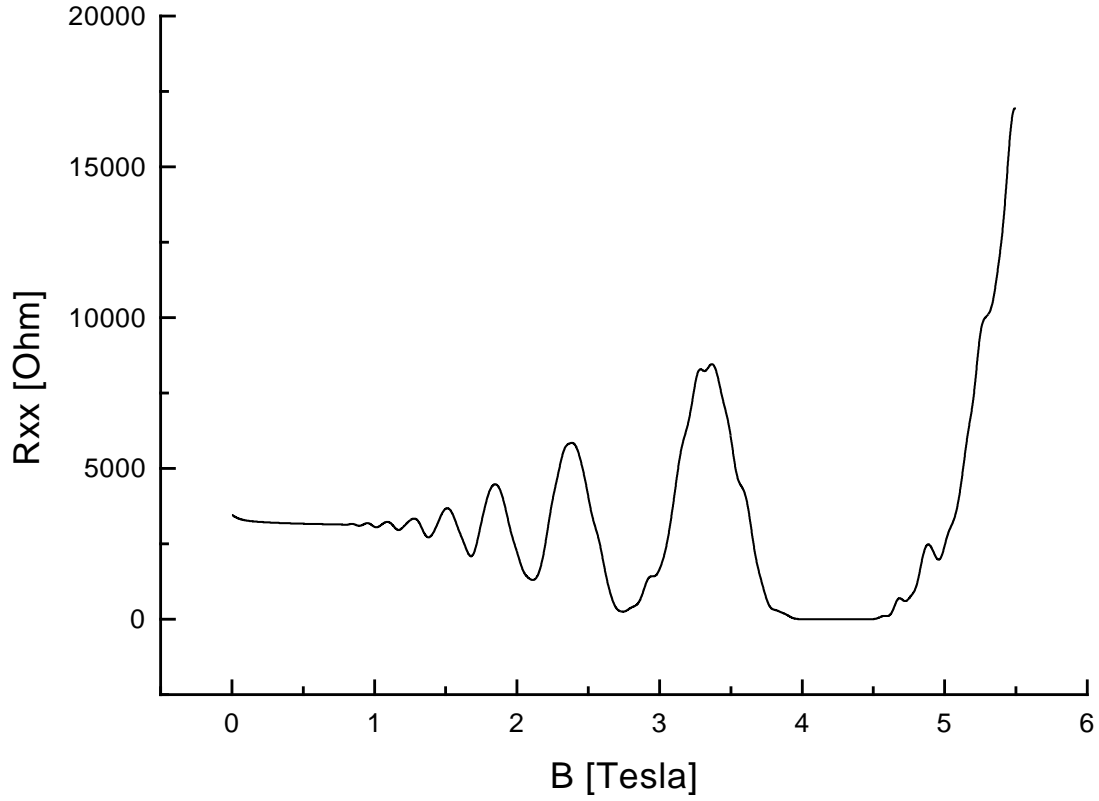
Figure 7: *Transversal* quantized HALL resistance (without spin degeneracy) down to filling factor $\nu = 1$. (Computer simulation based on a phenomenological formula *geometrically* averaging over $N = 1000$ replicas within a charge carrier density variance $\sigma = 3\,\%$ around $n_{2D} \approx 2.0 \cdot 10^{15}/\mathrm{m}^2$. Inhomogenities of the external magnetic field may be modelled in an analogous fashion.)

Figure 8: *Longitudinal* quantized HALL resistance (without spin degeneracy) down to filling factor $\nu = 1$. (Computer simulation based on a phenomenological formula *geometrically* averaging over $N = 1000$ replicas within a charge carrier density variance $\sigma = 3\,\%$ around $n_{2D} \approx 2.0 \cdot 10^{15}/\mathrm{m}^2$. Inhomogenities of the external magnetic field may be modelled in an analogous fashion.)

Figure 9: *Transversal* quantized HALL resistance (without spin degeneracy) down to filling factor $\nu = 1$. (Computer simulation based on a phenomenological formula *geometrically* averaging over $N = 1000$ replicas within a charge carrier density variance $\sigma = 6\,\%$ around $n_{2D} \approx 2.0 \cdot 10^{15}/\mathrm{m}^2$. Inhomogenities of the external magnetic field may be modelled in an analogous fashion.)

Figure 10: *Longitudinal* quantized HALL resistance (without spin degeneracy) down to filling factor $\nu = 1$. (Computer simulation based on a phenomenological formula *geometrically* averaging over $N = 1000$ replicas within a charge carrier density variance $\sigma = 6\,\%$ around $n_{2D} \approx 2.0 \cdot 10^{15}/\mathrm{m}^2$. Inhomogenities of the external magnetic field may be modelled in an analogous fashion.)

9 Figures: Sample geometry and topology
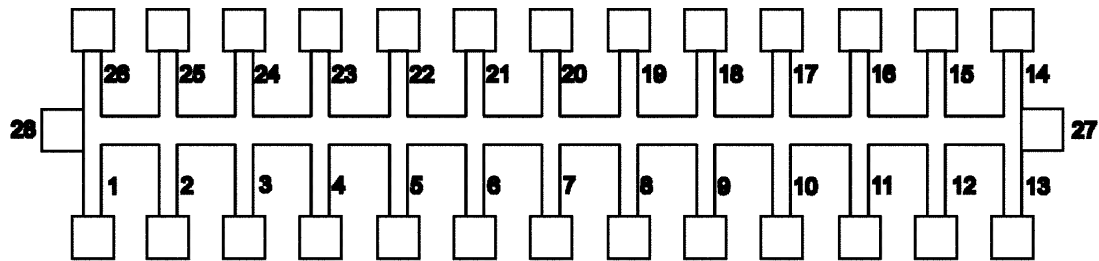
Figure 11: HALL-bar layout
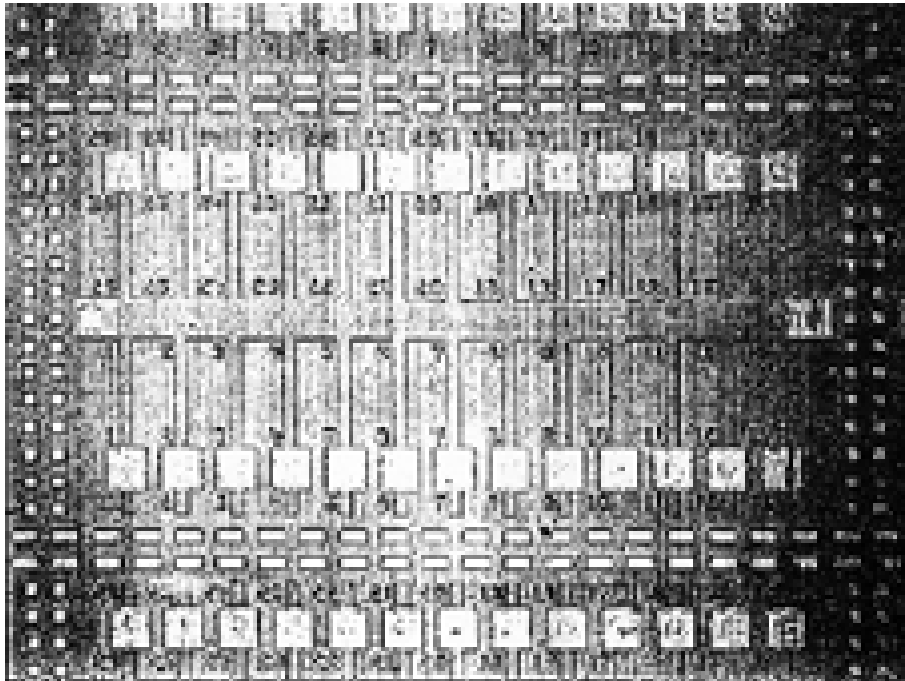
Figure 12: Photograph of the HALL-bar
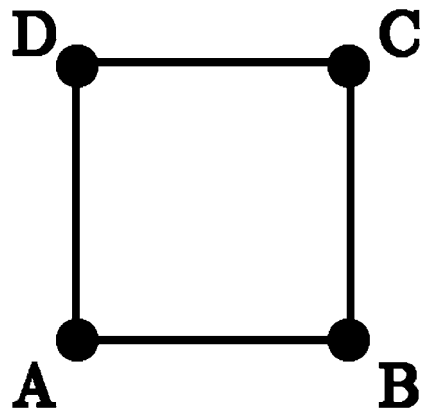
Figure 13: VAN DER PAUW-type sample layout
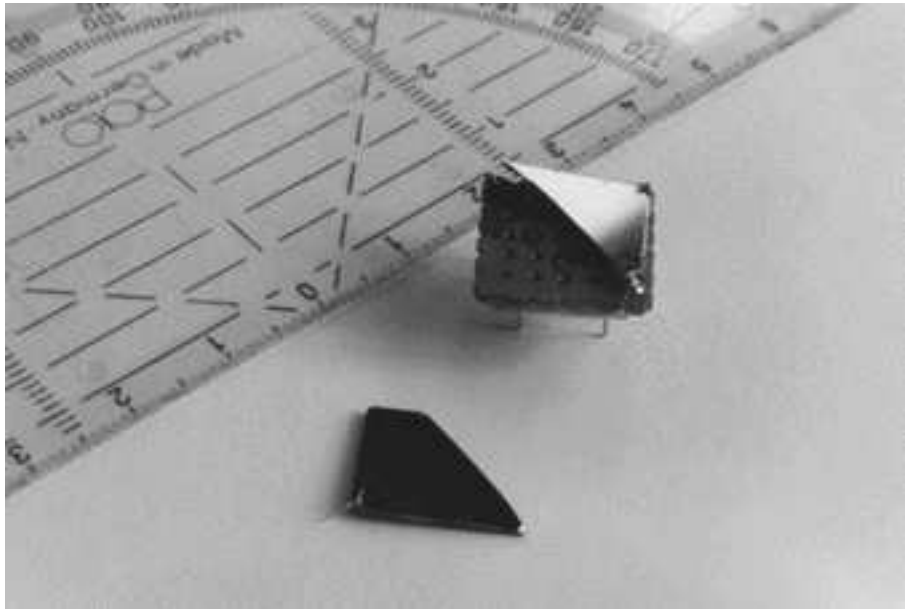
Figure 14: Photograph of the (broken) VAN DER PAUW-type "**centi**" sample
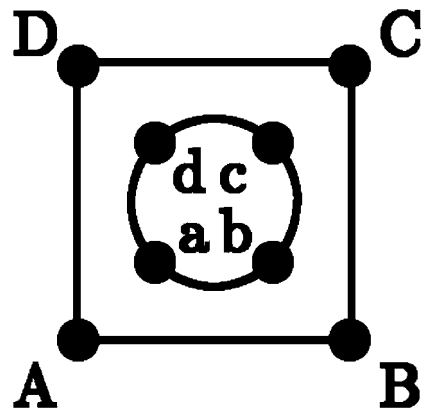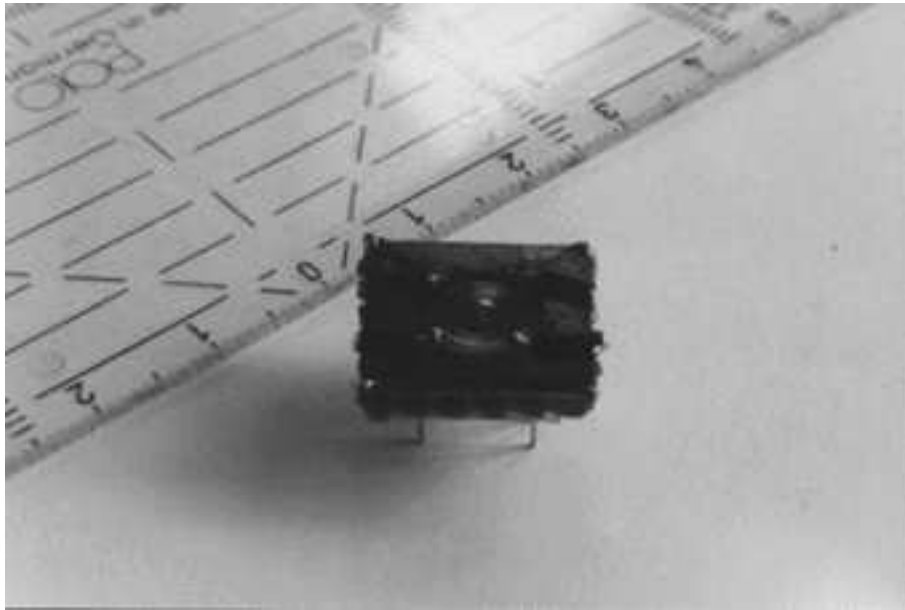
Figure 15: van der Pauw-Corbino-hybrid sample layout

Figure 16: Photograph of the VAN DER PAUW-CORBINO-hybrid sample
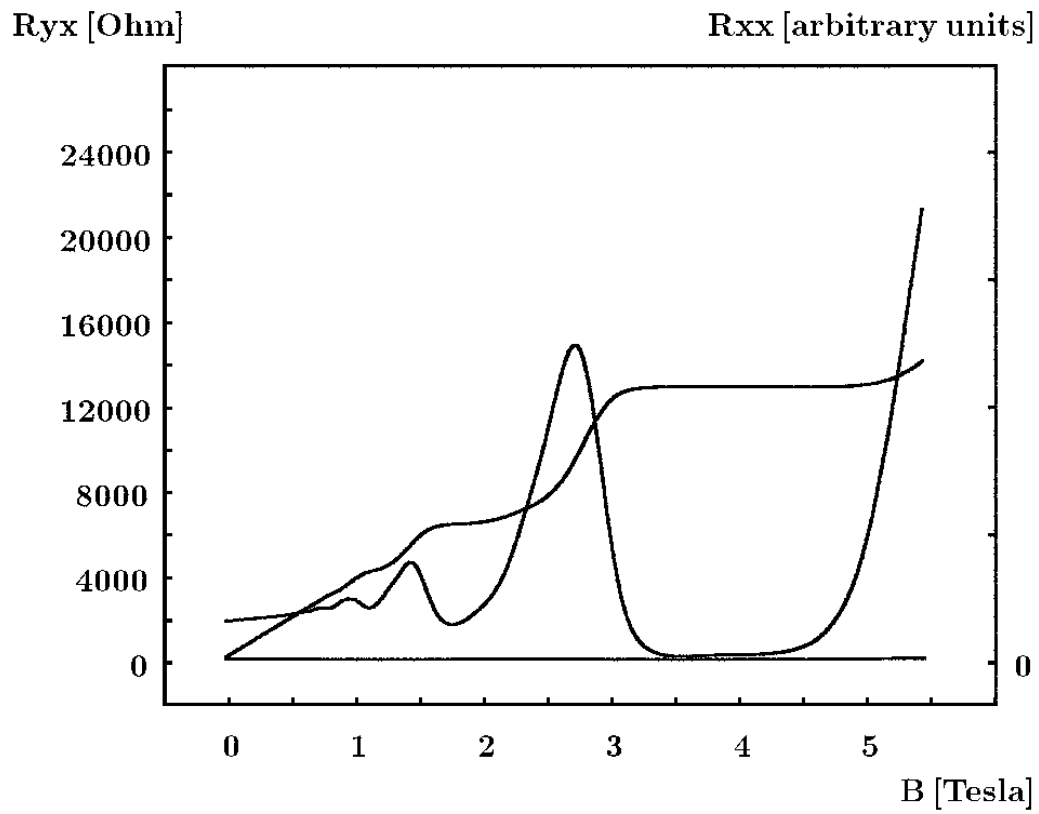
10 Figures: Experimental results

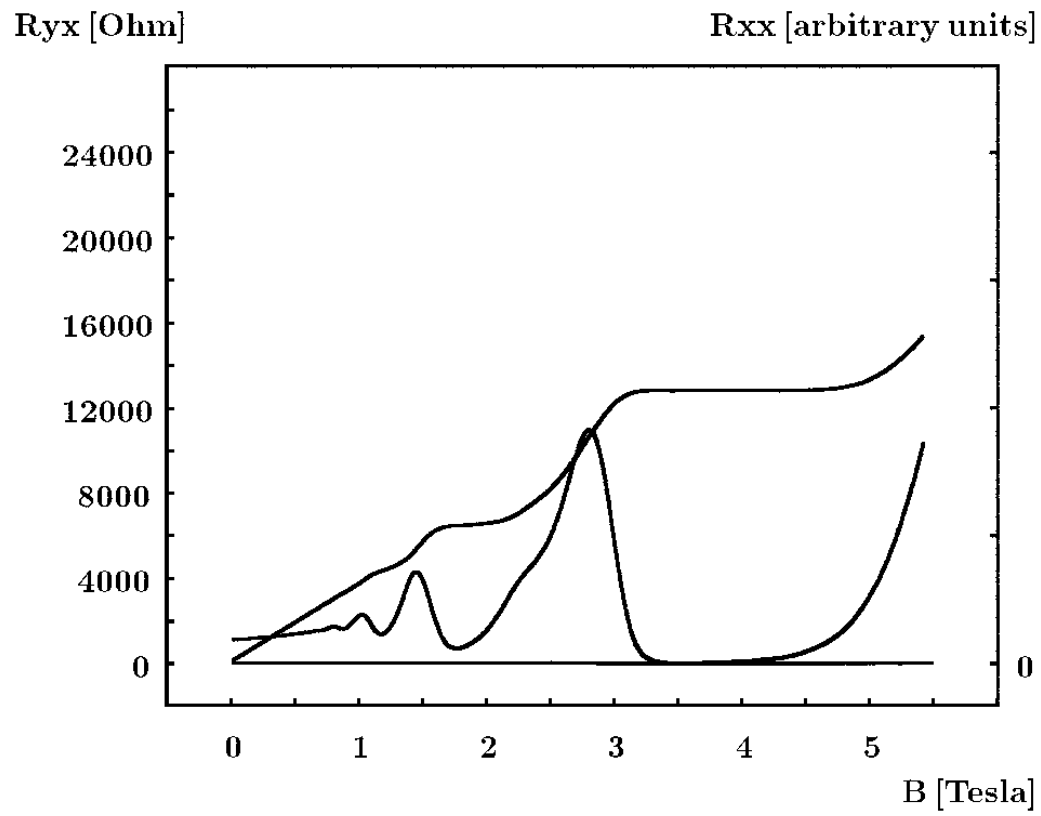Figure 17: Measurement 1 on the VAN DER PAUW-type "**centi**" sample
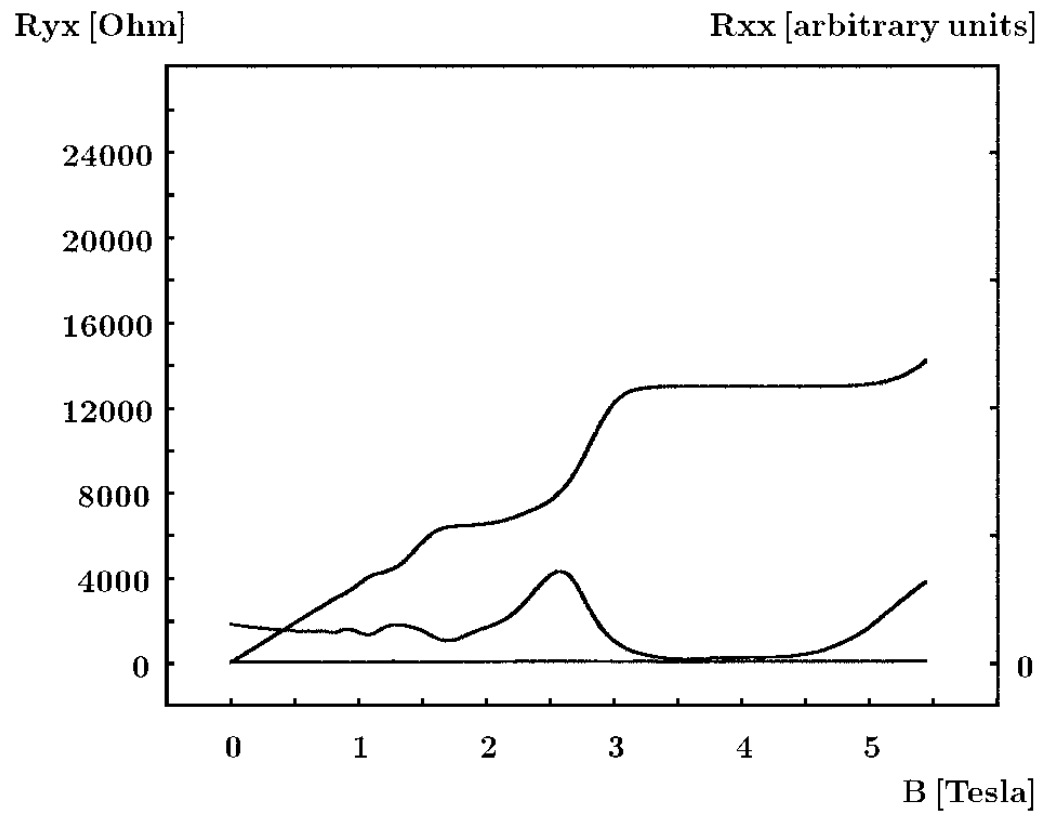
Figure 18: Measurement 2 on the VAN DER PAUW-type "**centi**" sample

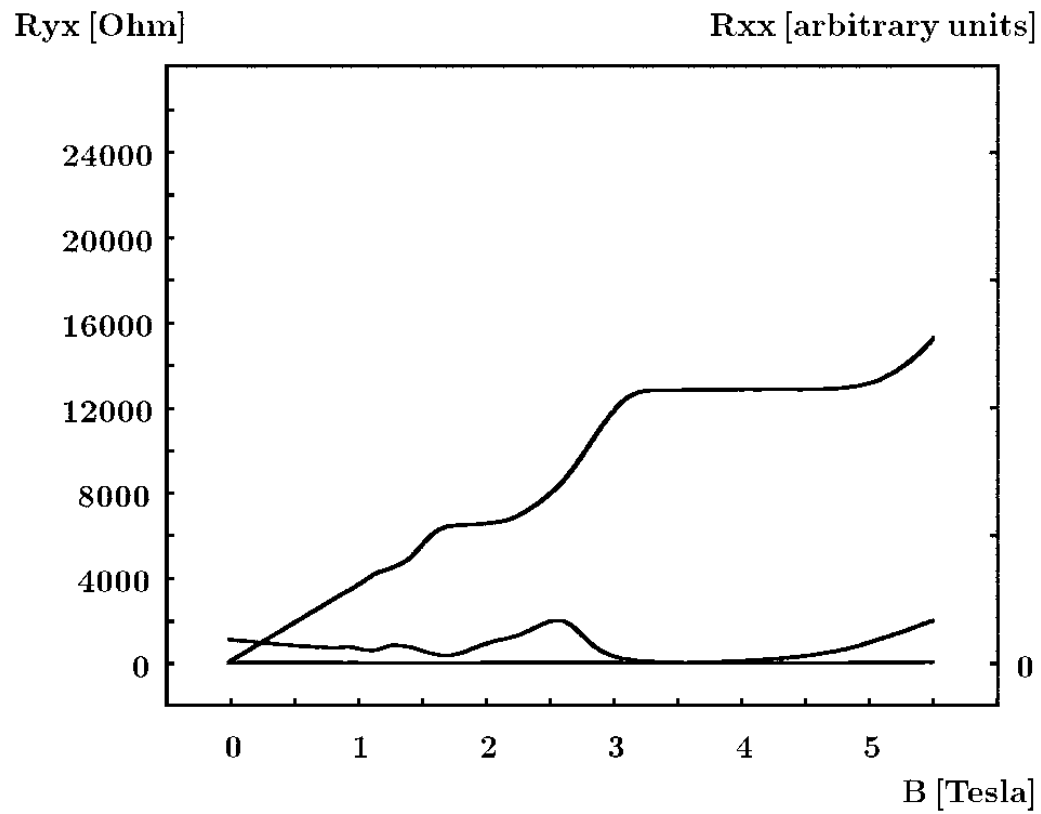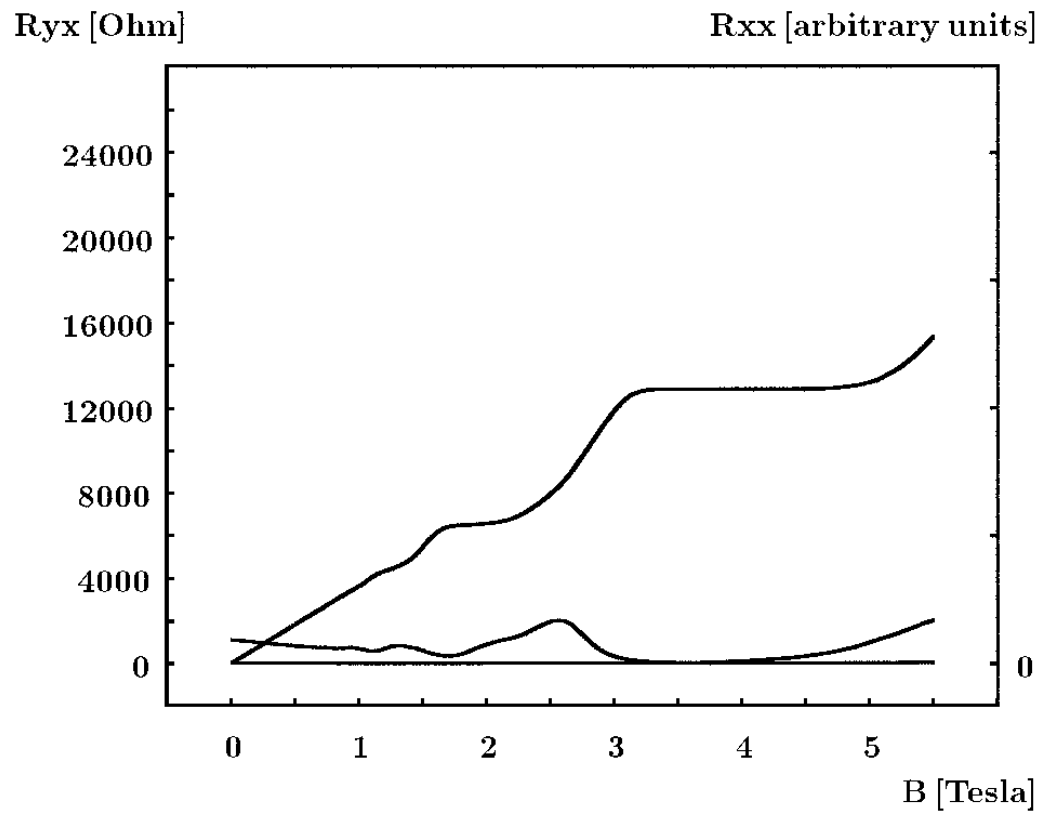Figure 19: Measurement 3 on the VAN DER PAUW-type "**centi**" sample

Ryx [Ohm]

Rxx [arbitrary units]

Figure 20: Measurement 4 on the VAN DER PAUW-type "**centi**" sample

Ryx [Ohm]   **Rxx [arbitrary units]**

Figure 21: Measurement 5 on the VAN DER PAUW-type "**centi**" sample

Ryx [Ohm]   **Rxx [arbitrary units]**
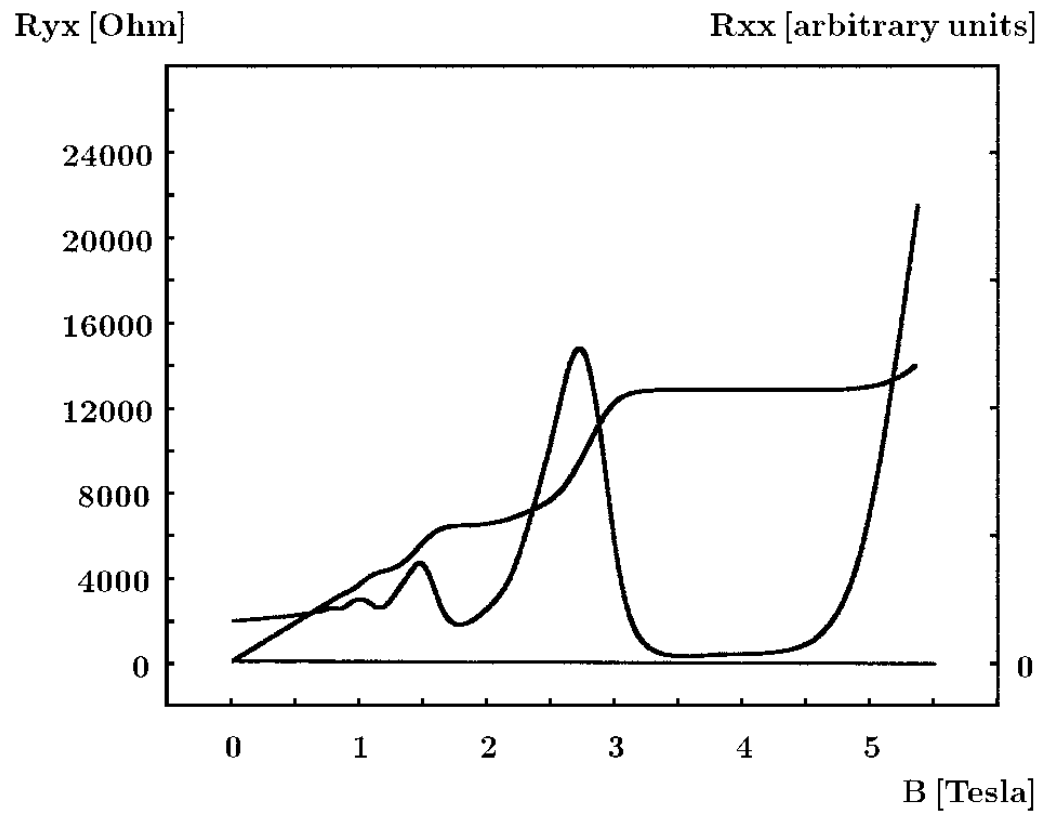

Figure 22: Measurement 6 on the VAN DER PAUW-type "**centi**" sample
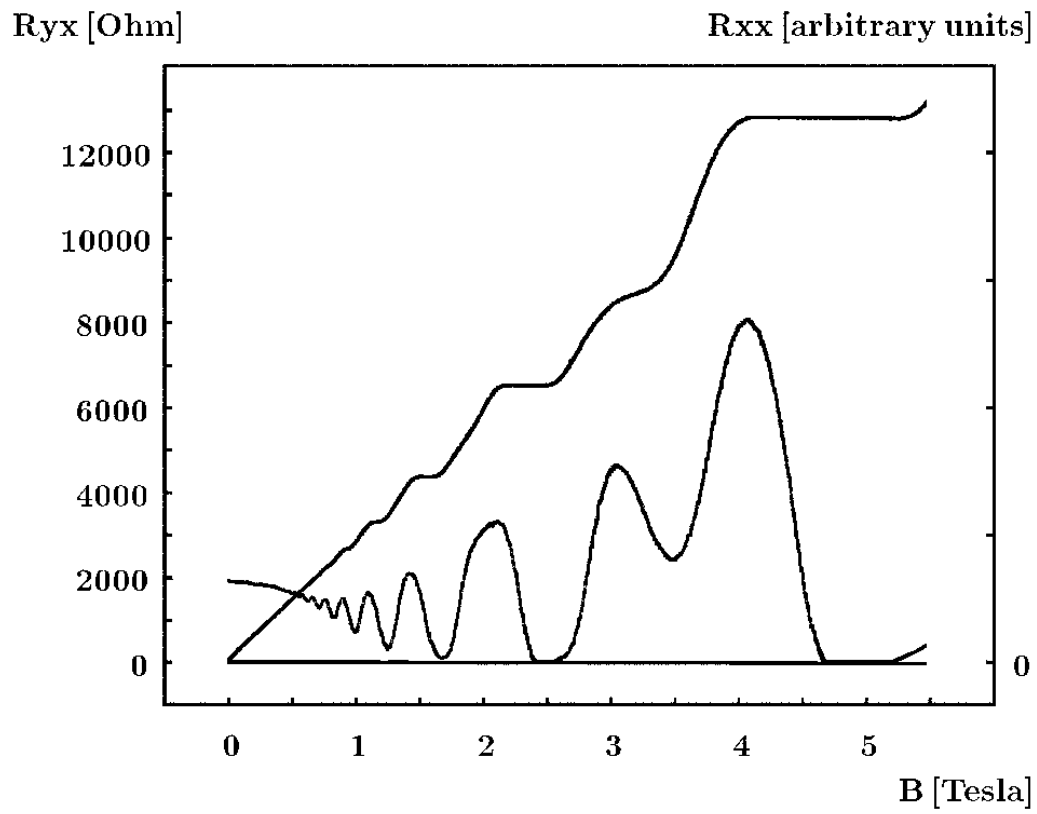
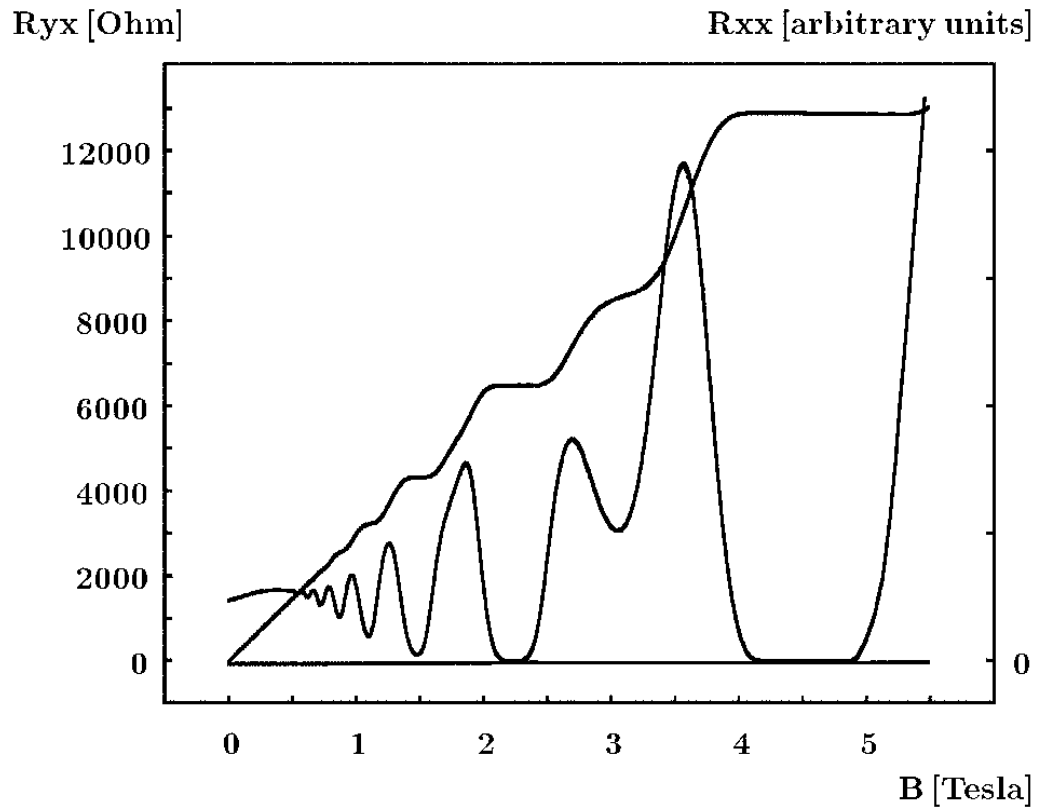Figure 23: Measurement on a HALL-bar-type "**micro**" sample

Ryx [Ohm]   **Rxx [arbitrary units]**

Figure 24: Measurement on a VAN DER PAUW-type "**milli**" sample

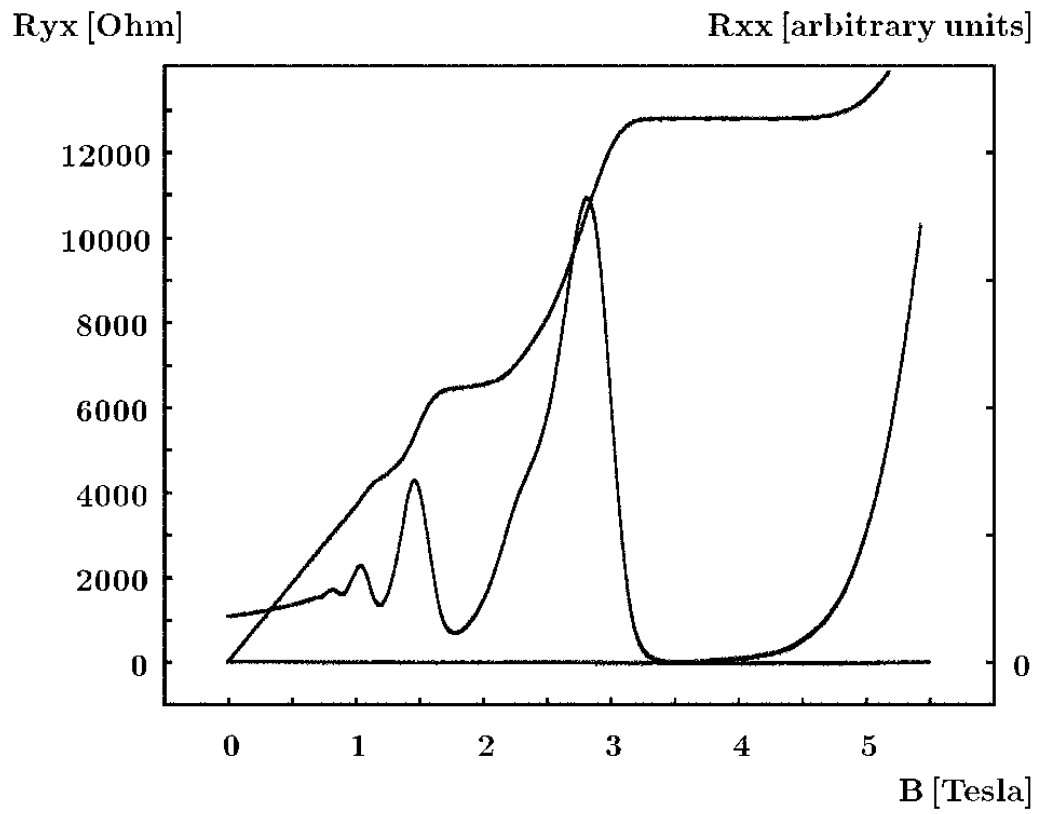**Ryx [Ohm]**   **Rxx [arbitrary units]**

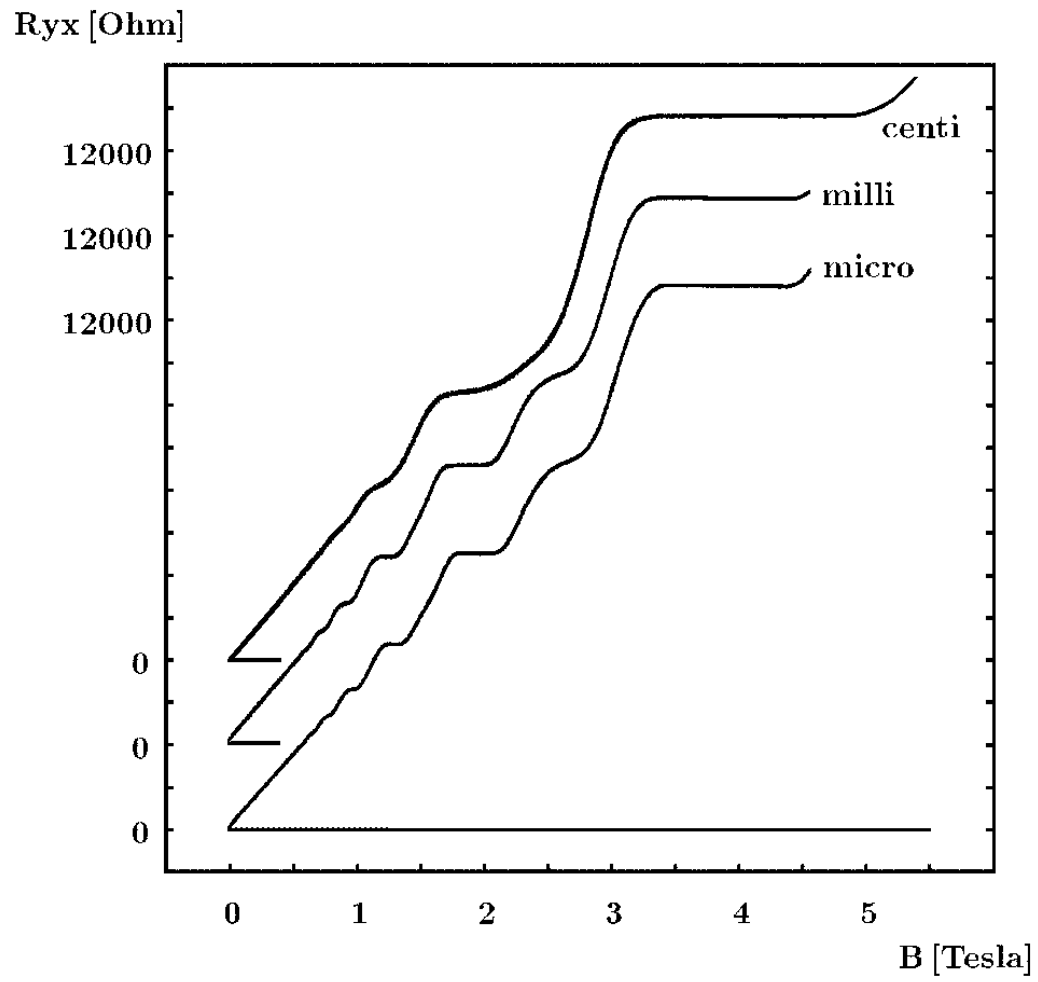Figure 25: Measurement on a VAN DER PAUW-type "**centi**" sample

Figure 26: Scaling in real space: Comparison of different sample sizes
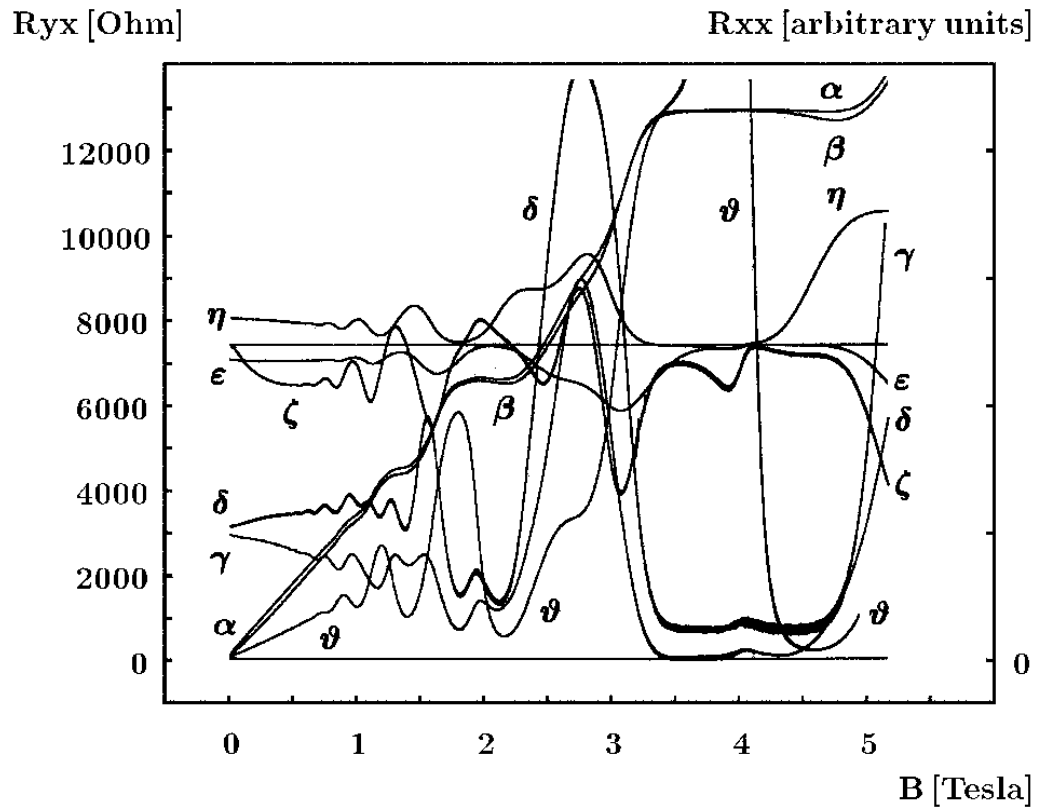
Figure 27: Measurement on a VAN DER PAUW-CORBINO-hybrid sample

11 Tables

ν	"micro"	"milli"	"centi"
2	100 %	121 %	179 %
3	100 %	150 %	50 %
4	100 %	117 %	150 %
6	100 %	117 %	100 %
8	100 %	117 %	50 %
10	100 %	100 %	0 %
12	100 %	100 %	0 %

Table 1: Relative plateau width in Fig. 26

meas. no.	time	I_{in}	U_{out}	U_{out} range
1	00:00	AC	BD	3 mV
		AB	CD	0.3 mV
2	00:20	BD	CA	3 mV
		BC	AD	0.3 mV
3	00:37	CA	DB	3 mV
		CD	AB	0.3 mV
4	00:45	DB	AC	3 mV
		DA	BC	0.3 mV
5	00:60	AC	BD	3 mV
		AB	CD	0.3 mV
6	01:31	AC	BD	3 mV
		AB	CD	0.3 mV

Table 2: Measurements depicted in Fig. 17 - Fig. 22

curve	I_{in}	U_{out}	U_{out} range	zero line	overall characteristics
$\boldsymbol{\alpha}$	AC	DB	3 mV	low	standard transversal curve
$\boldsymbol{\beta}$	ac	db	3 mV	low	standard transversal curve
$\boldsymbol{\gamma}$	AB	CD	0.3 mV	low	longitudinal curve with neg. slope
$\boldsymbol{\delta}$	ab	cd	0.3 mV	low	longitudinal curve with pos. slope
$\boldsymbol{\epsilon}$	AD	bd	3 mV	mid	longitudinal curve with pos. slope
$\boldsymbol{\zeta}$	AC	bd	0.3 mV	mid	curve with second derivative content
$\boldsymbol{\eta}$	AB	bd	3 mV	mid	longitudinal curve with neg. slope
$\boldsymbol{\vartheta}$	AC	bB	3 mV	low	hybrid curve

Table 3: Evaluation of Fig. 27